filament networks with alteration of cell shape and nuclear integrity. *J Invest Dermatol* 108:179–87

Deshpande R, Woods TL, Fu J *et al.* (2000) Biochemical characterization of S100A2 in human keratinocytes: subcellular localization, dimerization, and oxidative cross-linking. *J Invest Dermatol* 115: 477–85

Donato R (2001) S100: a multigenic family of calcium-modulated proteins of the EF-hand type with intracellular and extracellular functional roles. *Int J Biochem Cell Biol* 33:637–68

Eckert RL, Broome AM, Ruse M *et al.* (2004) S100 proteins in the epidermis. *J Invest Dermatol* 123:23–33

Elias PM, Ahn SK, Denda M *et al.* (2002) Modulations in epidermal calcium regulate the expression of differentiation-specific markers. *J Invest Dermatol* 119:1128–36

Han SY, Gai W, Yancovitz M *et al.* (2008) Nucleofection is a highly effective gene transfer technique for human melanoma cell lines. *Exp Dermatol* 17:405–11

Hohl D, Mehrel T, Lichti U *et al.* (1991) Characterization of human loricrin. Structure and function of a new class of epidermal cell envelope proteins. *J Biol Chem* 266:6626–36

Hudson JR Jr, Dawson EP, Rushing KL *et al.* (1997) The complete set of predicted genes from Saccharomyces cerevisiae in a readily usable form. *Genome Res* 7:1169–73

Ishida-Yamamoto A, Hohl D, Roop DR *et al.* (1993) Loricrin immunoreactivity in human skin: localization to specific granules (L-granules) in acrosyringia. *Arch Dermatol Res* 285:491–8

Ishida-Yamamoto A, Takahashi H, Presland RB *et al.* (1998) Translocation of profilaggrin N-terminal domain into keratinocyte nuclei with fragmented DNA in normal human skin and loricrin keratoderma. *Lab Invest* 78:1245–53

Kalinin A, Marekov LN, Steinert PM (2001) Assembly of the epidermal cornified cell envelope. *J Cell Sci* 114:3069–70

Kalinin AE, Kajava AV, Steinert PM (2002) Epithelial barrier function: assembly and structural features of the cornified cell envelope. *Bioessays* 24:789–800

Koch PJ, de Viragh PA, Scharer E *et al.* (2000) Lessons from loricrin-deficient mice: compensatory mechanisms maintaining skin barrier function in the absence of a major cornified envelope protein. *J Cell Biol* 151: 389–400

Kuechle MK, Thulin CD, Presland RB *et al.* (1999) Profilaggrin requires both linker and filaggrin peptide sequences to form granules: implications for profilaggrin processing *in vivo*. *J Invest Dermatol* 112:843–52

Mauro T, Bench G, Sidderas-Haddad E *et al.* (1998) Acute barrier perturbation abolishes the Ca^{2+} and K^{+} gradients in murine epidermis: quantitative measurement using PIXE. *J Invest Dermatol* 111:1198–201

Mehrel T, Hohl D, Rothnagel JA *et al.* (1990) Identification of a major keratinocyte cell envelope protein, loricrin. *Cell* 61:1103–12

Mildner M, Jin J, Eckhart L *et al.* (2010) Knockdown of filaggrin impairs diffusion barrier function and increases UV sensitivity in a human skin model. *J Invest Dermatol* 130:2286–94

Miyake S, Makimura M, Kanegae Y *et al.* (1996) Efficient generation of recombinant adenoviruses using adenovirus DNA-terminal protein complex and a cosmid bearing the full-length virus genome. *Proc Natl Acad Sci USA* 93:1320–4

Okada M, Hatakeyama T, Itoh H *et al.* (2004) S100A1 is a novel molecular chaperone and a member of the Hsp70/Hsp90 multichaperone complex. *J Biol Chem* 279:4221–33

O'Shaughnessy RF, Welti JC, Cooke JC *et al.* (2007) AKT-dependent HspB1 (Hsp27) activity in epidermal differentiation. *J Biol Chem* 282: 17297–305

Pearton DJ, Dale BA, Presland RB (2002) Functional analysis of the profilaggrin N-terminal peptide: identification of domains that regulate nuclear and cytoplasmic distribution. *J Invest Dermatol* 119:661–9

Pearton DJ, Nirunsuksiri W, Rehemtulla A *et al.* (2001) Proprotein convertase expression and localization in epidermis: evidence for multiple roles and substrates. *Exp Dermatol* 10:193–203

Presland RB, Bassuk JA, Kimball JR *et al.* (1995) Characterization of two distinct calcium-binding sites in the amino-terminus of human profilaggrin. *J Invest Dermatol* 104:218–23

Presland RB, Haydock PV, Fleckman P *et al.* (1992) Characterization of the human epidermal profilaggrin gene. Genomic organization and identification of an S-100-like calcium binding domain at the amino terminus. *J Biol Chem* 267:23772–81

Presland RB, Kimball JR, Kautsky MB *et al.* (1997) Evidence for specific proteolytic cleavage of the *N*-terminal domain of human profilaggrin during epidermal differentiation. *J Invest Dermatol* 108:170–8

Robinson NA, Lapic S, Welter JF *et al.* (1997) S100A11, S100A10, annexin I, desmosomal proteins, small proline-rich proteins, plaminogen activator inhibitor-2, and involucrin are components of the cornified envelope of cultured human epidermal keratinocytes. *J Biol Chem* 272:12035–46

Ruse M, Lambert A, Robinson N *et al.* (2001) S100A7, S100A10, and S100A11 are transglutaminase substrates. *Biochemistry* 40:3167–73

Sandilands A, Sutherland C, Irvine AD *et al.* (2009) Filaggrin in the frontline: role in skin barrier function and disease. *J Cell Sci* 122:1285–94

Steinert PM, Marekov LN (1995) The proteins elafin, filaggrin, keratin intermediate filaments, loricrin, and small proline-rich proteins 1 and 2 are isodipeptide cross-linked components of the human epidermal cornified cell envelope. *J Biol Chem* 270:17702–11

Steinert PM, Marekov LN (1997) Direct evidence that involucrin is a major early isopeptide cross-linked component of the keratinocyte cornified cell envelope. *J Biol Chem* 272:2021–30

Yoneda K, Akiyama M, Morita K *et al.* (1998) Expression of transglutaminase 1 in human hair follicles, sebaceous glands and sweat glands. *Br J Dermatol* 138:37–44

Yoneda K, Demitsu T, Manabe M *et al.* (2010a) Expression of wild-type, but not mutant, loricrin causes programmed cell death in HaCaT keratinocytes. *J Dermatol* 37:956–64

Yoneda K, Demitsu T, Nakai K *et al.* (2010b) Activation of vascular endothelial growth factor receptor 2 in a cellular model of loricrin keratoderma. *J Biol Chem* 285:16184–94

Yoneda K, Fujimoto T, Imamura S *et al.* (1990a) Distribution of fodrin in the keratinocyte *in vivo* and *in vitro*. *J Invest Dermatol* 94:724–9

Yoneda K, Fujimoto T, Imamura S *et al.* (1990b) Fodrin is localized in the cytoplasm of keratinocytes cultured in low calcium medium: immunoelectron microscopic study. *Acta Histochem Cytochem* 23:139–48

Yoneda K, Furukawa T, Zheng YJ *et al.* (2004) An autocrine/paracrine loop linking keratin 14 aggregates to tumor necrosis factor alpha-mediated cytotoxicity in a keratinocyte model of epidermolysis bullosa simplex. *J Biol Chem* 279:7296–303

Yoneda K, Hohl D, McBride OW *et al.* (1992a) The human loricrin gene. *J Biol Chem* 267:18060–6

Yoneda K, McBride OW, Korge BP *et al.* (1992b) The cornified cell envelope: loricrin and transglutaminases. *J Dermatol* 19:761–4

Yoneda K, Steinert PM (1993) Overexpression of human loricrin in transgenic mice produces a normal phenotype. *Proc Natl Acad Sci USA* 90:10754–8

Zhang T, Woods TL, Elder JT (2002) Differential responses of S100A2 to oxidative stress and increased intracellular calcium in normal, immortalized, and malignant human keratinocytes. *J Invest Dermatol* 119:1196–201

The American Journal of Pathology, Vol. 181, No. 3, September 2012

http://dx.doi.org/10.1016/j.ajpath.2012.06.005

Molecular Pathogenesis of Genetic and Inherited Diseases

Reduced Expression of Epidermal Growth Factor Receptor, E-Cadherin, and Occludin in the Skin of Flaky Tail Mice Is Due to Filaggrin and Loricrin Deficiencies

Kozo Nakai,* Kozo Yoneda,* Yoichiro Hosokawa,* Tetsuya Moriue,* Richard B. Presland,†‡ Padraic G. Fallon,§ Kenji Kabashima,¶ Hiroaki Kosaka,‖ and Yasuo Kubota*

From the Departments of Dermatology and Cardiovascular Physiology,‖ Faculty of Medicine, Kagawa University, Kagawa, Japan; the Division of Dermatology,† Department of Medicine, and the Department of Oral Health Sciences and Graduate Program in Oral Biology,‡ School of Dentistry, University of Washington, Seattle, Washington; the Institute of Molecular Medicine,§ Trinity College Dublin, Dublin, Ireland, United Kingdom; and the Department of Dermatology,¶ Graduate School of Medicine, Kyoto University, Kyoto, Japan*

Disruption of skin barrier function leads to increases in the percutaneous transfer of allergens and the incidence of atopic dermatitis. Flaky tail (*Flg^{ft}*) mice have been used as a model of atopic dermatitis with skin barrier dysfunction. Although *Flg^{ft}* mice are known to have filaggrin mutation, the mechanism responsible for the skin barrier dysfunction that they display needs to be determined, especially for the roles of epidermal adhesion and junction proteins. Herein, we report the decreased expression of epidermal growth factor receptor (EGFR), E-cadherin, occludin, and SIRT1 in the skin of *Flg^{ft}* mice, compared with those in C57BL/6J mice. Administration of N-acetyl-L-cysteine, an antioxidant, in the drinking water improved these protein expressions in the skin of *Flg^{ft}* mice. Notably, we discovered that loricrin expression was suppressed in *Flg^{ft}* mice. *In vitro* experiments showed that filaggrin small interfering RNA, loricrin small interfering RNA, or SIRT1 inhibitor sirtinol suppressed the expression levels of EGFR, E-cadherin, and occludin in a human immortalized keratinocyte cell line (HaCaT cells). Our findings suggest that the observed reductions in EGFR, E-cadherin, and occludin expression were due to filaggrin deficiency accompanied with subsequent loricrin deficiency and disruption of the SIRT1 pathway in the skin of *Flg^{ft}* mice. ***(Am J Pathol 2012, 181:969–977; http://dx.doi.org/10.1016/j.ajpath.2012.06.005)***

Recent reports have suggested that filaggrin is essential for skin barrier function which prevents the body from the entry of foreign substances that would otherwise trigger aberrant immune responses. Decreased filaggrin expression partially accounts for the impaired epidermal barrier observed in ichthyosis vulgaris and atopic dermatitis.[1] The disruption of skin barrier function due to filaggrin deficiency has been reported in studies that used flaky tail (*Flg^{ft}*) mice.[2–4] However, cellular pathogenesis of the skin barrier defects caused by the decreased filaggrin expression remains unclear.

Cell–cell interactions might have fundamental effects on the barrier function of the epidermis. The interactions are primarily mediated by four types of plasma membrane structure: gap junctions, tight junctions, desmosomes, and adherens junctions. Tight junctions, in which occludin[5] and claudins[6] are integral membrane proteins, act as important apical barriers that regulate paracellular permeability and separate the apical and basolateral membrane regions, thereby inducing polarity.[7–9] Adherens junctions and desmosomes mediate cell–cell adhesion via members of the cadherin family such as E-cadherin, which controls adherens junctions in the epidermis.[10] A recent study found defects in tight junction claudin-1 and claudin-23 expression in patients with atopic dermatitis.[11] The dissolution of tight junctions may be followed by the down-regulation of E-cadherin expression and the dissolution of adherens junctions,[12] which

Supported by the fund for Kagawa University Young Scientists 2011 and Grants-in-Aid for scientific research to K.N. from the Ministry of Education, Science, Sports, and Culture, Japan.

Accepted for publication June 7, 2012.

Address reprint requests to Kozo Nakai, M.D., Ph.D., Department of Dermatology, Faculty of Medicine, Kagawa University, 1750-1 Ikenobe, Miki-cho, Kita-gun, Kagawa, Japan 761-0793. E-mail: kozo@kms.ac.jp.

are concomitantly regulated with epidermal growth factor receptor (EGFR).[13] We hypothesized that these cell–cell interactions and EGFR expression could be disturbed by filaggrin deficiency. Silent mating type information regulation 2 homolog 1 (SIRT1) is a redox-sensitive nicotinamide adenine dinucleotide-dependent deacetylase that is modified by oxidants and carbonyl stress, and its deacetylase levels are decreased by aging and in chronic inflammatory conditions such as chronic obstructive pulmonary disease in which excess reactive oxygen species formation occurs.[14] Because SIRT1 is known to inhibit proliferation and to promote differentiation in *in vitro* skin keratinocytes,[15] SIRT1 can be concomitantly involved in the regulation of adhesion molecules and EGFR in skin keratinocytes. Because atopic dermatitis is a chronic inflammatory skin condition, it is also possible that SIRT1 expression is modified in the filaggrin-deficient skin of *Flg*^{ft} mice, which denote human atopic dermatitis.

In the present study, we examined whether the expression levels of EGFR, E-cadherin, occludin, and SIRT1 are reduced in *Flg*^{ft} mice, compared with expression levels in C57BL/6J (B6) mice. We next used an antioxidant, N-acetyl-L-cysteine (NAC), for the purpose of recovering these protein expressions by ameliorating inflammatory/oxidative conditions in the skin of *Flg*^{ft} mice. Because loricrin is a major protein of the epidermal cornified cell envelope, which is an essential structure for skin barrier function, and it has been reported that loricrin expression is down-regulated in patients with atopic dermatitis,[16] we examined whether the expression levels of loricrin are reduced or not in *Flg*^{ft} mice. Because *in vivo* skin is heterogeneous, and *Flg*^{ft} mouse is a mixed strain of filaggrin mutation and matted mutation, we examined the effects of filaggrin or loricrin knockdown with small interfering RNA (siRNA) on the protein expression levels of EGFR, E-cadherin, occludin, and SIRT1 in a human epidermal keratinocyte cell line (HaCaT cells). The effects of the SIRT1 inhibitor sirtinol were also examined.

Materials and Methods

Reagents and Antibodies

NAC, Dulbecco's modified Eagle's medium, PBS, and N^{ω}-nitro-L-arginine methyl ester (L-NAME) were obtained from Sigma-Aldrich (St. Louis, MO). AG1478 was purchased from Calbiochem-Novabiochem (San Diego, CA). Sirtinol was purchased from Enzo Life Sciences (Plymouth Meeting, PA). The antibodies against EGFR, E-cadherin, SIRT1, occludin, and β-actin were purchased from Cell Signaling Technology (Danvers, MA). The antibody against filaggrin was purchased from Santa Cruz Biotechnology Inc. (Santa Cruz, CA), loricrin was obtained from Covance (Emeryville, CA), and glyceraldehyde-3-phosphate dehydrogenase (GAPDH) was from EnoGene Biotech (New York, NY).

Mice

All animal experiments were conducted in accordance with the institutional guidelines for the care and use of laboratory animals. The *Flg*^{ft} mice were obtained from The Jackson Laboratory (Bar Harbor, ME), and the C57BL/6J (B6) mice were obtained from CLEA Japan (Megro, Tokyo, Japan). The mice were housed in a room at the Health Science Center of Kagawa University under controlled temperature (23°C) and humidity (55%) and specific pathogen free conditions. The mice had free access to water and chow (Oriental Yeast Co., Itabashi, Tokyo, Japan). We administered NAC dissolved in drinking water at a concentration of 7 mg/mL (neutralized to pH 7.4 with NaOH) to some *Flg*^{ft} mice from birth.[17] The rest of the *Flg*^{ft} mice and B6 mice served as the untreated group. At 8 weeks of age, the mice were anesthetized with intraperitoneal sodium pentobarbital (50 mg/kg) injection, and full-thickness sections of the dorsal skin were dissected. We obtained the skin of the neonatal and 8-week-old *Flg*^{ft} mice that were backcrossed five generations onto a B6 strain background from Kyoto University, Kyoto, Japan. We also obtained 8- to10-week-old *Flg*^{ft} mice that were backcrossed 10 generations onto a B6 strain background from Trinity College Dublin, Dublin, Ireland.

Histology and Immunohistochemical Analysis

Skin samples (1 to 2 cm^2) were removed from the middorsum of the sacrificed mice and fixed directly in 10% buffered formalin. The tissues were dehydrated and embedded in paraffin, and then 5-μm sections were cut, deparaffinized in xylene, rehydrated, and immunostained with primary antibodies with the use of the Histofine simple stain reagent (Nichirei, Tokyo, Japan), according to the manufacturer's protocol. Briefly, endogenous peroxidase activity was blocked by incubating the sections with 3% hydrogen peroxide for 5 minutes. After being washed with PBS, the sections were incubated with the primary antibodies at room temperature for 1 hour, washed in PBS, and then incubated with peroxidase-conjugated secondary antibodies. After being washed, the sections were incubated with 3-3′-diaminobenzidine tetrahydrochloride solution and counterstained with Mayer's hematoxylin. For the histologic portion of the study, skin sections were visualized with routine H&E staining.

Measurement of Serum and Skin Tissue TNFα/IL-6/IL-1β/IL-17/VEGF Concentration

Tumor necrosis factor (TNF)α/IL-6 levels in the mouse serum and skin tissue were determined by enzyme-linked immunosorbent assay (ELISA) kit of Gen-Probe Incorporated (San Diego, CA). IL-1β/IL-17 levels in the mouse serum and skin tissue were determined by ELISA Kit of RayBiotech Inc. (Norcross, GA). The vascular endothelial growth factor (VEGF) levels in the mouse serum and skin tissue were determined by Quantikine Mouse VEGF Immunoassay (R&D Systems, Minneapolis, MN). In accordance with the manufacturer's protocol, the avidin–horseradish peroxidase color reaction was measured by using a microplate reader. The values of skin tissue TNFα/IL-6/IL-1β/IL-17/VEGF concentration were normalized to the protein concentration of the skin tissue.

Cell Culture

HaCaT cells (a generous gift from Professor N.E. Fusenig, German Cancer Research Center, Heidelberg, Germany) were cultured in Dulbecco's modified Eagle's medium with 10% heat-inactivated fetal bovine serum at 37°C in a humidified atmosphere of 5% CO_2 and 95% air.[18]

HaCaT Cells Grown at the Air–Liquid Interface

For the raft culture studies, LabCyte EPI-MODEL (J-TEC, Gamagori, Aichi, Japan) was used with modification. Briefly, HaCaT cells were grown on cell culture inserts (0.4-μm pore diameter; BD, Franklin Lakes, NJ) in LabCyte EPI-MODEL assay medium. The cell culture inserts were placed in a 24-well plate that had been filled with the assay medium. The medium in the cell culture inserts was aspirated 24 hours later, and HaCaT cells were grown at the air–liquid interface. The medium in the 24-well plates was changed twice a week. Cells were cultured for 7 days.

siRNA Transfection

To knockdown filaggrin and loricrin in HaCaT cells, we used stealth siRNA (Invitrogen, Carlsbad, CA). Target sequences of the gene-specific stealth siRNA sequences were as indicated for filaggrin (NM-001016, nt1941, 5′-GAGGUGGUCUGGGUCUGCUUCCAGA-3′) and loricrin (NM-000427, nt31, 5′-GGCUCUCCUUCCUUCUCAGA-CAAGA-3′). The stealth siRNA transfection was performed according to the manufacturer's protocol. HaCaT cells were plated in 6-well plates. OPTI-MEM I Reduced Serum Medium (500 μL) was mixed with 5 μL of Lipofectamine 2000 and 5 μL of a 20-μmol/L stealth siRNA solution or the control RNA solution. After incubation at room temperature for 30 minutes, the solution was added to 1.5 mL of OPTI-MEM I Reduced Serum Medium and transfected to the HaCaT cells. HaCaT cells were then incubated for 24 hours before seeding onto cell culture inserts.

Cell Proliferation Assay

The cell proliferation assay was conducted with Cell Counting Kit-8 (Dojindo, Kumamoto, Japan), in which WST-8 (2-(2-methoxy-4-nitrophenyl)−3-(4-nitrophenyl)-5-(2,4-disulfophenyl)-2H-tetrazolium, monosodium salt) is converted to formazan by cellular dehydrogenase. The absorbance of formazan, which is proportional to the cell number, was determined at 450 nm.

Western Blot Analysis

Skin tissue specimens were homogenized with a Polytron homogenizer in RIPA buffer containing 1% v/v NP40, 20 mmol/L Tris (pH 7.7), 150 mmol/L NaCl, 1 mmol/L EDTA, and a mixture of protease inhibitors (Calbiochem, San Diego, CA). The cells were washed with PBS and then treated with RIPA buffer. After incubation at 4°C for 20 minutes, the samples were sonicated on ice and centrifuged at 14,000 rpm for 10 minutes. The protein concentrations of the supernatant fluids were analyzed with the bicinchoninic acid protein assay (Pierce, Rockford, IL). An equal amount of protein was separated on reducing NuPAGE 4% to 12% Bis-Tris or 7% Tris-acetate gel (Invitrogen) and transferred to a nitrocellulose membrane. Alternatively, the protein was separated on SDS-PAGE gel and transferred to a polyvinylidene difluoride membrane. The membrane was then probed with antibodies against various primary antibodies. The membrane-bound primary antibodies were visualized with appropriate secondary antibodies conjugated to horseradish peroxidase and a chemiluminescent substrate (Pierce). The immunoreactive signals from the chemiluminescent substrate were visualized by exposing them to standard x-ray films. The images were subjected to densitometric analysis with the use of Image J software verison 1.38 (NIH, Bethesda, MD).

qRT-PCR

Total RNA was extracted from skin tissue or cultured HaCaT cells with the use of TRIzol reagent (Invitrogen). Reverse transcription was performed with a high-capacity cDNA reverse transcription kit (Applied Biosystems, Foster City, CA). Quantitative RT-PCR (qRT-PCR) was performed with the Taqman gene expression assay system (Applied Biosystems). The probes used were Mm00433023_m1 (mouse EGFR), Mm01247357_m1 (mouse E-cadherin), Mm00500912_m1 (mouse occludin), Mm00490758_m1 (mouse SIRT1), Mm01219285_m1 (mouse loricrin), and Mm999999_g1 (mouse GAPDH). Probes for GAPDH were used as endogenous control. qRT-PCR was performed with an ABI 7500 Real-Time PCR System. Gene expression values were calculated on the basis of the comparative threshold cycle method, normalized to the expression values of GAPDH, and displayed as fold induction relative to control.

Statistical Analysis

Data are expressed as the mean ± SE. Statistical analysis was performed by analysis of variance, followed by the Student's *t*-test, Welch's *t*-test, or Mann–Whitney's *U*-test. *P* values of <0.05 were considered to denote statistical significance.

Results

Loricrin Protein Expression Is Decreased in the Skin of Flg^{ft} *Mice*

Apparent abnormal histologic changes were not observed in the dorsal skin of 8-week-old *Flg^{ft}* mice (Figure 1A, upper panels). However, the formation of N-terminal peptide (32 kDa) and filaggrin monomer (28 kDa) was barely detectable by Western blot analysis in the dorsal skin of *Flg^{ft}* mice compared with that in the B6 mice (Figure 1B) Immunohistologic analysis found the relative

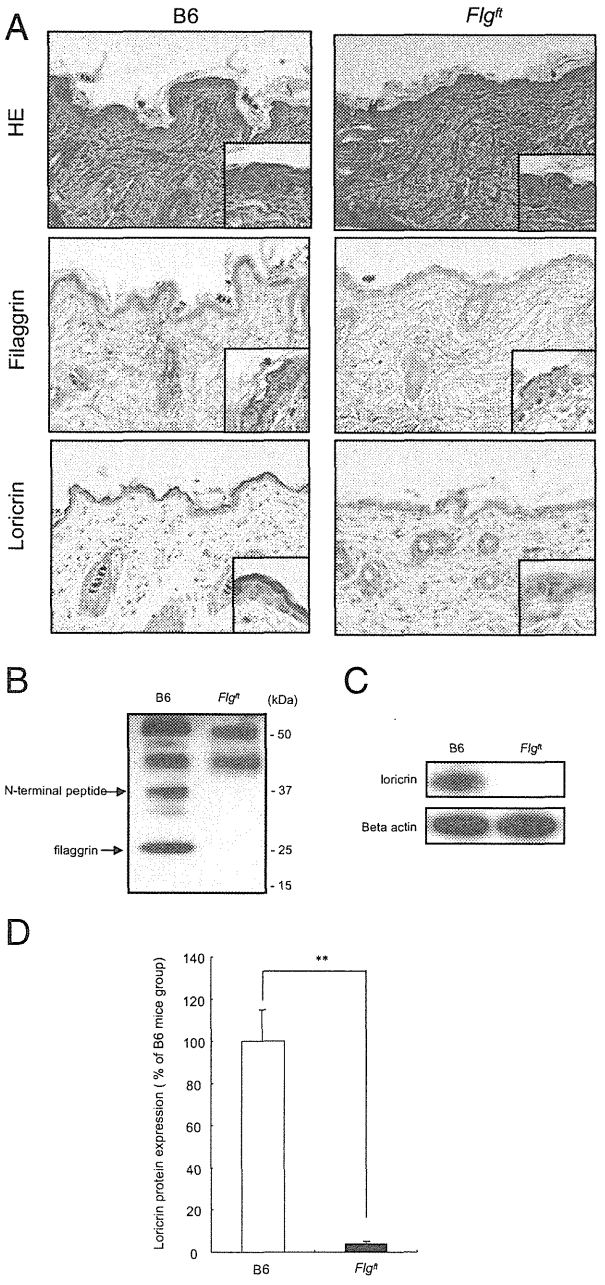

Figure 1. Loricrin expression was decreased in the skin of *Flg*^{ft} mice. **A:** Histology and immunohistochemistry of filaggrin and loricrin expression in the skin of *Flg*^{ft} mice and B6 mice. **B** and **C:** Western blot analysis of filaggrin, loricrin, and β-actin protein expression in the skin of *Flg*^{ft} mice and B6 mice. Representative results from four to seven mice per group are shown. **D:** The results of densitometric analysis are from pooled data. Values represent the mean ± SE (n = 3). $^{**}P < 0.005$ versus B6 mice.

absence of filaggrin in the epidermis of *Flg*^{ft} mice compared with that of the B6 mice (Figure 1A, middle panels). Unexpectedly, loricrin protein expression was barely detectable by Western blot analysis in the dorsal skin of *Flg*^{ft} mice compared with that of B6 mice (Figure 1, C and D). Immunohistologic analysis found the complete absence of loricrin from the epidermis of *Flg*^{ft} mice compared with that of B6 mice (Figure 1A, bottom panels).

EGFR, E-Cadherin, SIRT1, and Occludin Expression Are Suppressed in the Skin of Flg^{ft} *Mice*

We have recently reported that the expression of a gain-of-function mutant loricrin caused activation of EGFR in a cellular model of loricrin keratoderma.[19] Conversely, we hypothesized that a decrease in the expression of loricrin protein would affect the expression of EGFR. As shown in Figure 2B, we found that the expression of EGFR protein was suppressed in the dorsal skin of *Flg*^{ft} mice compared with that of age-matched B6 mice. Immunohistologic analysis found the relative absence of EGFR from the epidermis of *Flg*^{ft} mice compared with that of age-matched B6 mice (Figure 2A, upper panels). E-cadherin, a cell adhesion molecule, has been reported to associate/cooperate with EGFR to modulate the proliferation and differentiation of keratinocytes.[13] Western blot analysis found that the expression of E-cadherin protein was suppressed in the dorsal skin of *Flg*^{ft} mice compared with that of age-matched B6 mice (Figure 2B). Immunohistologic analysis found the relative absence of E-cadherin from the epidermis of *Flg*^{ft} mice compared with that of age-matched B6 mice (Figure 2A). As for the expression of the tight junction molecule occludin, its protein level was suppressed in the dorsal skin of *Flg*^{ft} mice compared

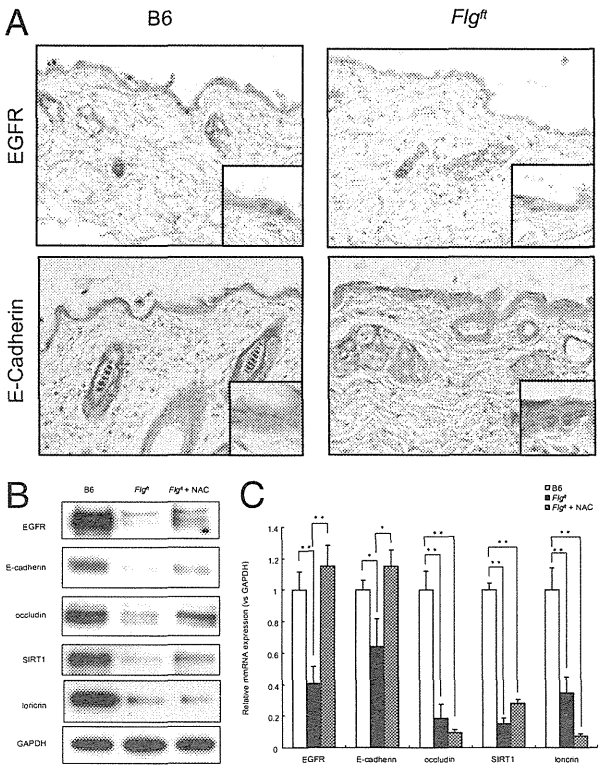

Figure 2. NAC restored the suppressed EGFR, E-cadherin, SIRT1, and occludin expression in the skin of *Flg*^{ft} mice. NAC (7 mg/mL) dissolved in drinking water was administered to *Flg*^{ft} mice from birth for 8 weeks. **A:** Immunohistochemistry of EGFR and E-cadherin expression in the skin of *Flg*^{ft} mice and B6 mice. **B:** Western blot analysis of EGFR, E-cadherin, occludin, SIRT1, and GAPDH protein expression in the skin of *Flg*^{ft} mice and B6 mice. **C:** qRT-PCR analysis of EGFR, E-cadherin, occludin, SIRT1, and GAPDH mRNA expression in the skin of *Flg*^{ft} mice and B6 mice (n = 4 to 5). $^{*}P < 0.05$, $^{**}P < 0.005$ versus B6 untreated mice.

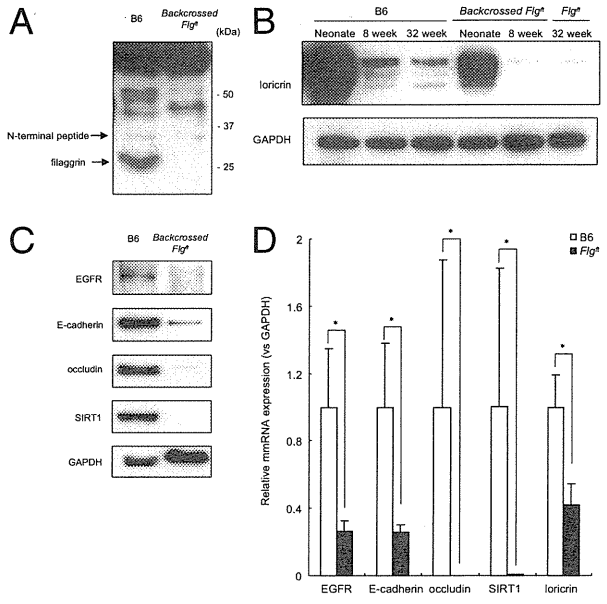

Figure 3. Loricrin, EGFR, E-cadherin, SIRT1, and occludin expressions were suppressed in the skin of backcrossed *Flg*^{ft} mice. **A** and **B:** Western blot analysis of filaggrin, loricrin, and GAPDH protein expression in the skin of backcrossed *Flg*^{ft} mice and B6 mice. Representative results from four mice per group are shown. **C:** Western blot analysis of EGFR, E-cadherin, occludin, SIRT1, and GAPDH protein expression in the skin of backcrossed *Flg*^{ft} mice and B6 mice. Representative results from four mice per group are shown. **D:** qRT-PCR analysis of EGFR, E-cadherin, occludin, SIRT1, and GAPDH mRNA expression in the skin of backcrossed *Flg*^{ft} mice and B6 mice ($n = 4$). $^{*}P < 0.05$ versus B6 mice.

with the age-matched B6 mice, as shown in Figure 2B. SIRT1 protein expression was also suppressed in the skin of *Flg*^{ft} mice (Figure 2B). As shown in Figure 2C, mRNA expression of EGFR, E-cadherin, occludin, SIRT1, and loricrin was suppressed in the skin of *Flg*^{ft} mice. Reduced SIRT1 expression indicated deranged inflammation and/or oxidative stress.[14] To ameliorate the inflammatory/oxidative condition in the skin, we administrated NAC water, an antioxidant solution, to *Flg*^{ft} mice. Notably, NAC supplementation for 8 weeks partially restored EGFR, E-cadherin, occludin, and SIRT1 protein expression in *Flg*^{ft} mice (Figure 2B). However, NAC did not restore loricrin protein expression (Figure 2B) and occludin, SIRT1, and loricrin mRNA expression (Figure 2C).

Loricrin, EGFR, E-Cadherin, SIRT1, and Occludin Expression Are Suppressed in the Skin of Backcrossed Flg^{ft} *Mice*

To exclude the issue of variable genetic background of *Flg*^{ft} mice, we examined the skin of *Flg*^{ft} mice that were backcrossed to B6 mice. The formation of N-terminal peptide (32 kDa) was reduced, and the formation of filaggrin monomer (28 kDa) was barely detectable in the dorsal skin of 8-week-old backcrossed *Flg*^{ft} mice compared with that in the B6 mice (Figure 3A). The high expression levels of loricrin were detected in the skin of neonatal backcrossed *Flg*^{ft} mice, but the expression levels were markedly reduced in 8-week-old backcrossed *Flg*^{ft} mice compared with B6 mice (Figure 3B). As shown in Figure 3C, protein expression of EGFR, E-cadherin, occludin, SIRT1, and loricrin was suppressed in the skin of 8-week-old backcrossed *Flg*^{ft} mice compared with that in the B6 mice. In addition, mRNA expression of EGFR, E-cadherin, occludin, SIRT1, and loricrin was suppressed in the skin of 8-week-old backcrossed *Flg*^{ft} mice compared with that in the B6 mice (Figure 3D). These results are consistent with those of non-backcrossed *Flg*^{ft} mice.

NAC Do Not Alter Proinflammatory Cytokines but Increases VEGF in the Skin of Flg^{ft} *Mice*

To examine the effects of NAC on immune status, we measured TNFα, IL-6, IL-1β, and IL-17 protein levels in the serum and the skin of *Flg*^{ft} mice. The serum protein levels of TNFα, IL-6, and IL-1β were below the detection limits of ELISA in both *Flg*^{ft} and B6 mice. The serum IL-17 protein levels and the skin tissue TNFα/IL-1β protein levels were significantly increased in *Flg*^{ft} mice compared with B6 mice. However, NAC did not alter these proinflammatory cytokine levels in the serum and the skin of the *Flg*^{ft} mice (Figure 4, A and B). VEGF interacts with EGFR and other related molecules in human epidermal keratinocytes.[19] NAC supplementation significantly increased the VEGF concentration in the skin of *Flg*^{ft} mice (Figure 4C).

Filaggrin siRNA and Loricrin siRNA Suppress the Expression Levels of EGFR, E-Cadherin, Occludin, and SIRT1 in HaCaT Cells Grown at the Air–Liquid Interface

Generally, *in vivo* skin is heterogeneous, and *Flg*^{ft} mouse is a mixed strain of filaggrin mutation plus matted mutation. We therefore performed *in vitro* experiments by using a human epidermal keratinocyte cell line (HaCaT cells). We cultured HaCaT cells at the air–liquid interface, where HaCaT cells can differentiate and develop a multilayered epithelium. We knocked down filaggrin or loricrin expression in HaCaT cells with siRNA. As shown in Figure 4, A and B, filaggrin siRNA inhibited the expression of loricrin as well as filaggrin in HaCaT cells grown at the air–liquid interface. However, loricrin siRNA blocked loricrin protein expression without affecting filaggrin protein expression in HaCaT cells grown at the air–liquid interface (Figure 5, A and B). Both filaggrin siRNA and loricrin siRNA reduced the protein expression levels of EGFR, E-cadherin, occludin, and SIRT1 in HaCaT cells grown at the air–liquid interface (Figure 5, C and D). These results indicate that the reduced protein expression of EGFR, E-cadherin, SIRT1, and occludin was due to loricrin deficiency, which was inducible by filaggrin deficiency.

SIRT1 Inhibition Decreases the Expression of EGFR and E-Cadherin in Monolayer Cultured HaCaT Cells

Because SIRT1 is known to inhibit proliferation and to promote differentiation,[15] we hypothesized that SIRT1 is

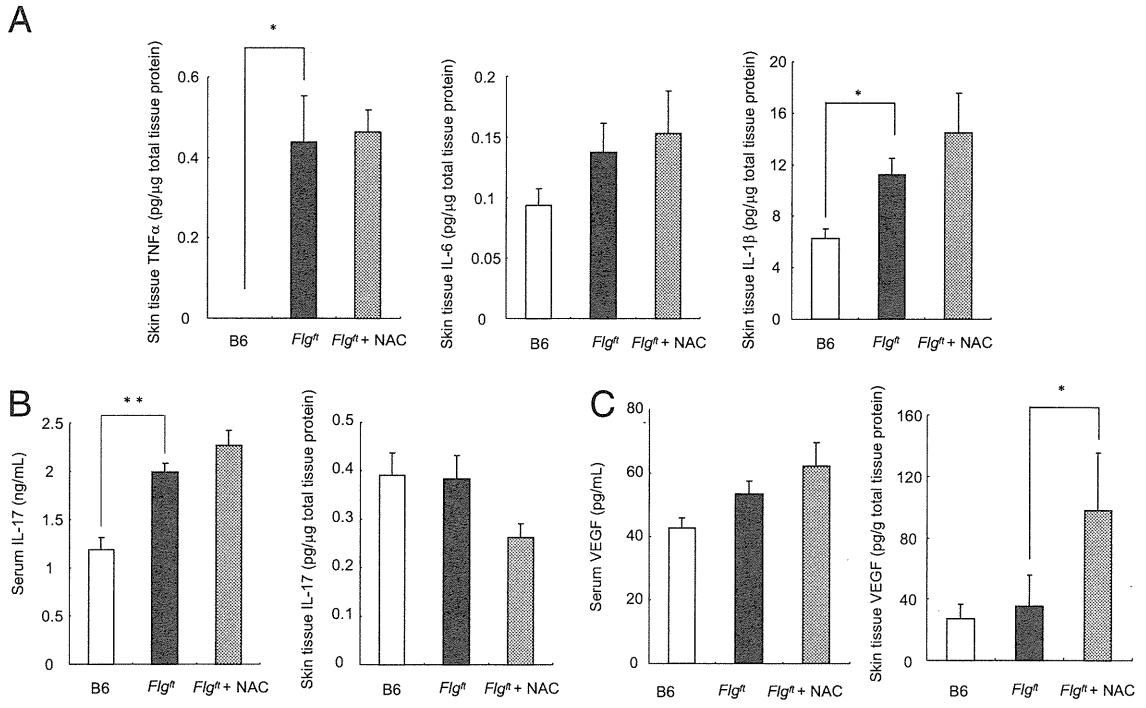

Figure 4. NAC did not alter proinflammatory cytokines but increased VEGF in the skin of *Flg*^{ft} mice. **A:** TNFα, IL-6, and IL-1β levels in the skin tissue of mice were determined by the sandwich ELISA method. These cytokines were not detected in the serum of mice. **B** and **C:** IL-17 and VEGF levels in the serum and skin tissue homogenate of mice were determined by the sandwich ELISA method. The tissue levels of cytokines and VEGF were normalized for the protein concentration of the skin tissue. Values represent the mean ± SE ($n = 4$). $^*P < 0.05$, $^{**}P < 0.005$ versus B6 untreated mice.

involved in the adherens and EGFR expression of epidermal keratinocytes. To verify our hypothesis, we investigated whether sirtinol, a SIRT1 inhibitor, altered the expression of EGFR and E-cadherin in HaCaT cells. The EGFR inhibitor AG1478 (10 μmol/L) suppressed the protein expression levels of EGFR and E-cadherin in monolayer cultured HaCaT cells (Figure 6, A and B), suggesting that AG1478 suppressed E-cadherin expression by inhibiting EGFR activity and expression. Similarly, sirtinol (100 μmol/L) suppressed the protein expression levels of EGFR and E-cadherin in monolayer cultured HaCaT cells. We further examined the effects of sirtinol on the cellular proliferation of monolayer cultured HaCaT cells. As shown in Figure 6C, HaCaT cells that were treated with AG1478 (10 μmol/L) for 48 hours displayed reduced proliferation. Similar effects were observed in the HaCaT cells treated with sirtinol (100 μmol/L), suggesting that SIRT1 is involved in the proliferation of HaCaT cells. Although nitric oxide might interfere with EGFR or E-cadherin expression, L-NAME (1 mmol/L), a nitric oxide synthase inhibitor, did not affect the

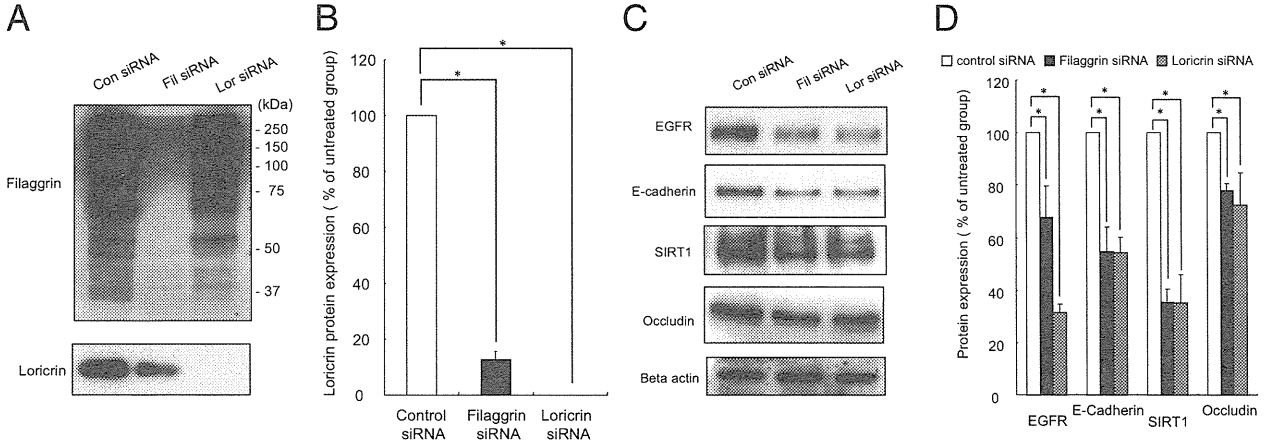

Figure 5. Filaggrin siRNA and loricrin siRNA suppressed the expression of EGFR and E-cadherin in HaCaT cells grown at the air–liquid interface. HaCaT cells were transfected with filaggrin, loricrin, or control siRNA and were grown at the air–liquid interface for 7 days. Protein expressions were analyzed by Western blot analysis. **A** and **C:** Representative results are shown. **B** and **D:** The densitometric analysis results were obtained from pooled data. Values represent the mean ± SE ($n = 3$). $^*P < 0.05$ versus control siRNA group.

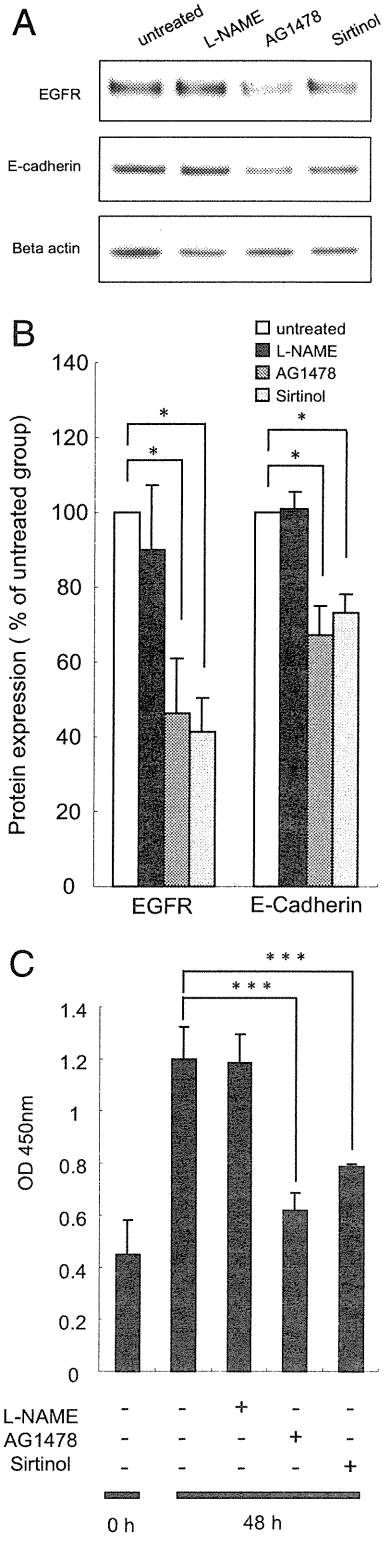

Figure 6. SIRT1 inhibition decreased the expression of EGFR and E-cadherin in monolayer cultured HaCaT cells. HaCaT cells were treated with L-NAME (1 mmol/L), AG1478 (10 μmol/L), or sirtinol (100 μmol/L) for 24 hours. Protein expressions were analyzed by Western blot analysis. **A:** Representative results are shown. **B:** The densitometric analysis results were obtained from pooled data. Values represent the mean ± SE ($n = 6$). **C:** HaCaT cells were treated with L-NAME (1 mmol/L), AG1478 (10 μmol/L), or sirtinol (100 μmol/L) for 24 hours. Cell number was assessed with a Cell Counting Kit-8. Values represent the mean ± SD ($n = 6$). $^{*}P < 0.05$, $^{***}P < 0.0005$ versus the untreated group.

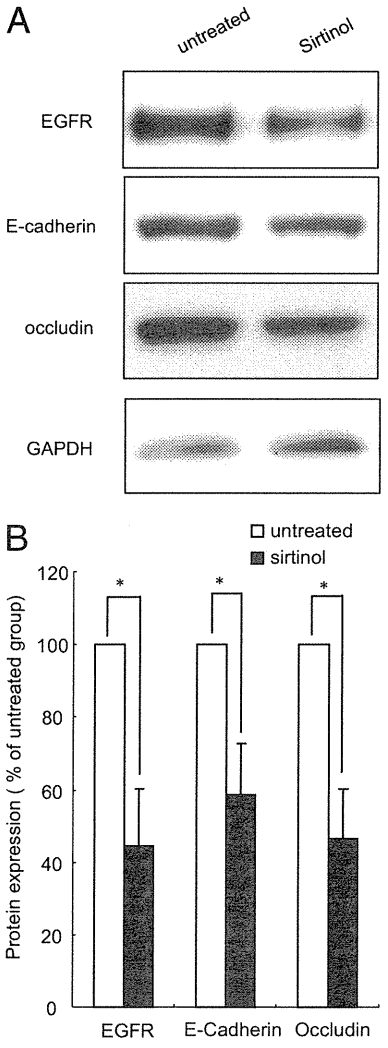

Figure 7. SIRT1 inhibition decreased the expression of EGFR, E-cadherin, and occludin in HaCaT cells grown at the air–liquid interface. HaCaT cells were grown at the air–liquid interface for 7 days. The medium with or without sirtinol (100 μmol/L) was changed twice a week. Protein expressions were analyzed by Western blot analysis. **A:** Representative results are shown. **B:** The densitometric analysis results were obtained from pooled data. Values represent the mean ± SE ($n = 6$). $^{*}P < 0.05$ versus the untreated group.

expression levels of these proteins (Figure 6, A and B) or proliferation (Figure 6C) in HaCaT cells.

SIRT1 Inhibition Decreases the Expression of Occludin in HaCaT Cells Grown at the Air–Liquid Interface

We next investigated the effects of sirtinol on differentiating HaCaT cells by culturing the cells at the air–liquid interface. Sirtinol (100 μmol/L) suppressed occludin expression in HaCaT cells grown at the air–liquid interface (Figure 7, A and B).Sirtinol (100 μmol/L) also suppressed EGFR and E-cadherin expression in HaCaT cells grown at the air–liquid interface (Figure 7, A and B). These results suggest that SIRT1 affects occludin expression in differentiating epidermal keratinocytes.

Discussion

It is generally accepted that atopic dermatitis is caused partially by the induction of skin barrier disruption due to decreased filaggrin expression. To examine the mechanism by which filaggrin deficiency compromises skin barrier, we investigated the expression of cellular junction-related proteins in *Flg*^{ft} mice, a model of atopic dermatitis with skin barrier dysfunction. As a result, we observed decreased EGFR, E-cadherin, occludin, and SIRT1 expression in *Flg*^{ft} mice. NAC supplementation partially restored the expression of these proteins in *Flg*^{ft} mice. To the best of our knowledge, we found for the first time that loricrin expression was suppressed in *Flg*^{ft} mice. *In vitro* experiments found that filaggrin siRNA, loricrin siRNA, and the SIRT1 inhibitor sirtinol suppressed the expression of EGFR, E-cadherin, and occludin in HaCaT cells. Filaggrin siRNA inhibited the expression of loricrin as well as filaggrin in HaCaT cells grown at the air–liquid interface, although loricrin siRNA did not block filaggrin protein expression.

Flg^{ft} mice arose spontaneously in 1958 at The Jackson Laboratory and were first reported in 1972.[20] A filaggrin deficiency in their epidermis was found in 2000.[21] Recent reports have suggested that *Flg*^{ft} mice display different phenotypes. Some *Flg*^{ft} mice show spontaneous dermatitis in the absence of treatments such as allergen administration,[4] whereas others have no dermatitis.[2,3] We did not find any abnormal histologic changes in the dorsal skin of 8-week-old *Flg*^{ft} mice. Moniaga et al[4] suggested that these discrepancies depend on the presence of the matted mutation or variations in the genetic backgrounds of the different strains used as well as on environmental factors.

Previously, Presland et al[21] reported that loricrin expression was slightly increased in the skin of newborn *Flg*^{ft} mice compared with that of B6 mice. In the present study, we found that the expression levels of loricrin were decreased in the dorsal skin of 8-week-old *Flg*^{ft} mice. Although no reports have suggested that loricrin expression is decreased in patients with ichthyosis vulgaris, it has been reported that loricrin expression was decreased in both the lesional and nonlesional skin of patients with atopic dermatitis.[16] Therefore, the down-regulation of loricrin expression could be a key step in atopic dermatitis deterioration due to filaggrin deficiency. Because previous reports have found that TNFα or type 2 helper T-cell cytokines suppressed loricrin mRNA expression,[16,22] loricrin might be reduced by these factors in *Flg*^{ft} mice.

Tight junctions exist just below the stratum corneum and regulate the paracellular permeability of the epidermis. De Benedetto et al[11] reported that the expression of the tight junction proteins claudin-1 and claudin-23 is reduced in patients with atopic dermatitis. Gruber et al[23] reported the reduced expression of the tight junction proteins occludin and ZO-1 in filaggrin-deficient human skin. We have found here that the expression levels of the tight junction protein occludin and the adherens junction protein E-cadherin were suppressed in the skin of *Flg*^{ft} mice. Because molecular cross talk between E-cadherin and EGFR has been reported in human NCI-H292 airway epithelial cells[24] and HaCaT cells,[25] we examined EGFR expression and found that it was decreased in the skin of *Flg*^{ft} mice. We further found that the SIRT1 expression was decreased in the skin of *Flg*^{ft} mice.

NAC partially restored EGFR, E-cadherin, occludin, and SIRT1 protein expression in the skin of *Flg*^{ft} mice. NAC also restored EGFR and E-cadherin mRNA expression in the skin of *Flg*^{ft} mice. The biological effects of NAC on the skin might include antioxidant and anti-inflammatory effects as well as the modulation of redox signaling pathways.[26] Although NAC has been reported to modify immunoreactions,[27] in our study, TNFα, IL-6, IL-1β, and IL-17 concentrations were not altered by NAC in the skin and the serum of *Flg*^{ft} mice. Considering that NAC restored SIRT1 expression in the skin of *Flg*^{ft} mice, NAC might increase VEGF, EGFR, E-cadherin, occludin, and SIRT1 by reducing the levels of oxidative stress in the skin of *Flg*^{ft} mice. Other possible effects of NAC have been suggested in clinical reports. The favorable therapeutic effects of topical NAC against lamellar ichthyosis suggest that NAC directly improves filaggrin-related skin barrier dysfunction[28] because patients with lamellar ichthyosis display abnormal keratinization due to mutations in their transglutaminase 1 gene and a differential pattern of filaggrin expression.

We could not conclude that the reduced protein expressions observed in *Flg*^{ft} mice were completely due to filaggrin deficiency, because *Flg*^{ft} mice are a mixed strain of filaggrin mutation plus matted mutation. We therefore performed *in vitro* siRNA experiments to gain insights into the molecular mechanisms responsible for the suppressed expression of EGFR, E-cadherin, SIRT1, and occludin in epidermis. Monolayer cultured HaCaT cells represent subbasal spinous keratinocytes, but they can develop a multilayered epithelium such as subcorneal keratinocytes when cultured at the air–liquid interface. Our results suggest that loricrin, which needs filaggrin for its expression, is required for the EGFR, SIRT1, E-cadherin, and occludin expressions in human skin epidermis. Our results also suggest that SIRT1 is required for the expressions of EGFR, E-cadherin, and occludin in human skin epidermis.

In summary, we have shown that loricrin, EGFR, E-cadherin, occludin, and SIRT1 expression were down-regulated in *Flg*^{ft} mice. We also performed *in vitro* experiments, which provided a mechanism for the skin barrier dysfunction observed in atopic dermatitis. NAC supplementation reversed the observed reductions in the expression levels of the above-mentioned proteins in *Flg*^{ft} mice, indicating that NAC could be considered as a therapeutic agent to restore the impaired barrier function of filaggrin-deficient skin.

Acknowledgments

We thank Fumiko Nishiyama and Miho Kato for their technical help.

References

1. Hudson TJ: Skin barrier function and allergic risk. Nat Genet 2006, 38:399–400
2. Fallon PG, Sasaki T, Sandilands A, Campbell LE, Saundèrs SP, Mangan NE, Callanan JJ, Kawasaki H, Shiohama A, Kubo A, Sundberg JP, Presland RB, Fleckman P, Shimizu N, Kudoh J, Irvine AD, Amagai M, McLean WH: A homozygous frameshift mutation in the mouse Flg gene facilitates enhanced percutaneous allergen priming. Nat Genet 2009, 41:602–608
3. Scharschmidt TC, Man MQ, Hatano Y, Crumrine D, Gunathilake R, Sundberg JP, Silva KA, Mauro TM, Hupe M, Cho S, Wu Y, Celli A, Schmuth M, Feingold KR, Elias PM: Filaggrin deficiency confers a paracellular barrier abnormality that reduces inflammatory thresholds to irritants and haptens. J Allergy Clin Immunol 2009, 124:496–506, 506 e491-496
4. Moniaga CS, Egawa G, Kawasaki H, Hara-Chikuma M, Honda T, Tanizaki H, Nakajima S, Otsuka A, Matsuoka H, Kubo A, Sakabe J, Tokura Y, Miyachi Y, Amagai M, Kabashima K: Flaky tail mouse denotes human atopic dermatitis in the steady state and by topical application with Dermatophagoides pteronyssinus extract. Am J Pathol 2010, 176:2385–2393
5. Furuse M, Hirase T, Itoh M, Nagafuchi A, Yonemura S, Tsukita S: Occludin: a novel integral membrane protein localizing at tight junctions. J Cell Biol 1993, 123:1777–1788
6. Furuse M, Fujita K, Hiiragi T, Fujimoto K, Tsukita S: Claudin-1 and −2: novel integral membrane proteins localizing at tight junctions with no sequence similarity to occludin. J Cell Biol 1998, 141:1539–1550
7. Anderson JM, Van Itallie CM: Tight junctions and the molecular basis for regulation of paracellular permeability. Am J Physiol 1995, 269: G467–G475
8. Tsukita S, Furuse M, Itoh M: Molecular dissection of tight junctions. Cell Struct Funct 1996, 21:381–385
9. Citi S: The molecular organization of tight junctions. J Cell Biol 1993, 121:485–489
10. Young P, Boussadia O, Halfter H, Grose R, Berger P, Leone DP, Robenek H, Charnay P, Kemler R, Suter U: E-cadherin controls adherens junctions in the epidermis and the renewal of hair follicles. EMBO J 2003, 22:5723–5733
11. De Benedetto A, Rafaels NM, McGirt LY, Ivanov AI, Georas SN, Cheadle C, Berger AE, Zhang K, Vidyasagar S, Yoshida T, Boguniewicz M, Hata T, Schneider LC, Hanifin JM, Gallo RL, Novak N, Weidinger S, Beaty TH, Leung DY, Barnes KC, Beck LA: Tight junction defects in patients with atopic dermatitis. J Allergy Clin Immunol 2011, 127:773–786e771-777
12. Thiery JP, Sleeman JP: Complex networks orchestrate epithelial-mesenchymal transitions. Nat Rev Mol Cell Biol 2006, 7:131–142
13. Muller EJ, Williamson L, Kolly C, Suter MM: Outside-in signaling through integrins and cadherins: a central mechanism to control epidermal growth and differentiation? J Invest Dermatol 2008, 128: 501–516
14. Caito S, Rajendrasozhan S, Cook S, Chung S, Yao H, Friedman AE, Brookes PS, Rahman I: SIRT1 is a redox-sensitive deacetylase that is post-translationally modified by oxidants and carbonyl stress. FASEB J 2010, 24:3145–3159
15. Blander G, Bhimavarapu A, Mammone T, Maes D, Elliston K, Reich C, Matsui MS, Guarente L, Loureiro JJ: SIRT1 promotes differentiation of normal human keratinocytes. J Invest Dermatol 2009, 129:41–49
16. Kim BE, Leung DY, Boguniewicz M, Howell MD: Loricrin and involucrin expression is down-regulated by Th2 cytokines through STAT-6. Clin Immunol 2008, 126:332–337
17. Cotter MA, Thomas J, Cassidy P, Robinette K, Jenkins N, Florell SR, Leachman S, Samlowski WE, Grossman D: N-acetylcysteine protects melanocytes against oxidative stress/damage and delays onset of ultraviolet-induced melanoma in mice. Clin Cancer Res 2007, 13: 5952–5958
18. Boukamp P, Petrussevska RT, Breitkreutz D, Hornung J, Markham A, Fusenig NE: Normal keratinization in a spontaneously immortalized aneuploid human keratinocyte cell line. J Cell Biol 1988, 106:761–771
19. Yoneda K, Demitsu T, Nakai K, Moriue T, Ogawa W, Igarashi J, Kosaka H, Kubota Y: Activation of vascular endothelial growth factor receptor 2 in a cellular model of loricrin keratoderma. J Biol Chem 2010, 285:16184–16194
20. Lane PW: Two new mutations in linkage group XVI of the house mouse. Flaky tail and varitint-waddler-J. J Hered 1972, 63:135–140
21. Presland RB, Boggess D, Lewis SP, Hull C, Fleckman P, Sundberg JP: Loss of normal profilaggrin and filaggrin in flaky tail (ft/ft) mice: an animal model for the filaggrin-deficient skin disease ichthyosis vulgaris. J Invest Dermatol 2000, 115:1072–1081
22. Kim BE, Howell MD, Guttman E, Gilleaudeau PM, Cardinale IR, Boguniewicz M, Krueger JG, Leung DY: TNF-alpha downregulates filaggrin and loricrin through c-Jun N-terminal kinase: role for TNF-alpha antagonists to improve skin barrier. J Invest Dermatol 2011, 131: 1272–1279
23. Gruber R, Elias PM, Crumrine D, Lin TK, Brandner JM, Hachem JP, Presland RB, Fleckman P, Janecke AR, Sandilands A, McLean WH, Fritsch PO, Mildner M, Tschachler E, Schmuth M: Filaggrin genotype in ichthyosis vulgaris predicts abnormalities in epidermal structure and function. Am J Pathol 2011, 178:2252–2263
24. Kim S, Schein AJ, Nadel JA: E-cadherin promotes EGFR-mediated cell differentiation and MUC5AC mucin expression in cultured human airway epithelial cells. Am J Physiol Lung Cell Mol Physiol 2005, 289:L1049–L1060
25. Pece S, Gutkind JS: Signaling from E-cadherins to the MAPK pathway by the recruitment and activation of epidermal growth factor receptors upon cell-cell contact formation. J Biol Chem 2000, 275:41227–41233
26. Parasassi T, Brunelli R, Costa G, De Spirito M, Krasnowska E, Lundeberg T, Pittaluga E, Ursini F: Thiol redox transitions in cell signaling: a lesson from N-acetylcysteine. ScientificWorldJournal 2010, 10: 1192–1202
27. Bengtsson A, Lundberg M, Avila-Carino J, Jacobsson G, Holmgren A, Scheynius A: Thiols decrease cytokine levels and down-regulate the expression of CD30 on human allergen-specific T helper (Th) 0 and Th2 cells. Clin Exp Immunol 2001, 123:350–360
28. Redondo P, Bauza A: Topical N-acetylcysteine for lamellar ichthyosis. Lancet 1999, 354:1880

Am J Physiol Cell Physiol 304: C790–C800, 2013.
First published February 20, 2013; doi:10.1152/ajpcell.00268.2012.

Dexamethasone induces caveolin-1 in vascular endothelial cells: implications for attenuated responses to VEGF

Junsuke Igarashi,[1] Takeshi Hashimoto,[1] Kazuyo Shoji,[2] Kozo Yoneda,[2] Ikuko Tsukamoto,[3] Tetsuya Moriue,[2] Yasuo Kubota,[2] and Hiroaki Kosaka[1]

[1]*Department of Cardiovascular Physiology, Kagawa University, Kagawa, Japan;* [2]*Department of Dermatology, Kagawa University, Kagawa, Japan; and* [3]*Department of Pharmaco-Bio-Informatics, Faculty of Medicine, Kagawa University, Kagawa, Japan*

Submitted 10 August 2012; accepted in final form 14 February 2013

Igarashi J, Hashimoto T, Shoji K, Yoneda K, Tsukamoto I, Moriue T, Kubota Y, Kosaka H. Dexamethasone induces caveolin-1 in vascular endothelial cells: implications for attenuated responses to VEGF. *Am J Physiol Cell Physiol* 304: C790–C800, 2013. First published February 20, 2013; doi:10.1152/ajpcell.00268.2012.—Steroids exert direct actions on cardiovascular cells, although underlying molecular mechanisms remain incompletely understood. We examined if steroids modulate abundance of caveolin-1, a regulatory protein of cell-surface receptor pathways that regulates the magnitudes of endothelial response to vascular endothelial growth factor (VEGF). Dexamethasone, a synthetic glucocorticoid, induces caveolin-1 at both levels of protein and mRNA in a time- and dose-dependent manner in pharmacologically relevant concentrations in cultured bovine aortic endothelial cells. Aldosterone, a mineralocorticoid, but not the sex steroids 17β-estradiol, testosterone, or progesterone, elicits similar caveolin-1 induction. Caveolin-1 induction by dexamethasone and that by aldosterone were abrogated by RU-486, an inhibitor of glucocorticoid receptor, and by spironolactone, a mineralocorticoid receptor inhibitor, respectively. Dexamethasone attenuates VEGF-induced responses at the levels of protein kinases Akt and ERK1/2, small-G protein Rac1, nitric oxide production, and migration. When induction of caveolin-1 by dexamethasone is attenuated either by genetically by transient transfection with small interfering RNA or pharmacologically by RU-486, kinase responses to VEGF are rescued. Dexamethasone also increases expression of caveolin-1 protein in cultured human umbilical vein endothelial cells, associated with attenuated tube formation responses of these cells when cocultured with normal fibroblasts. Immunohistochemical analyses revealed that intraperitoneal injection of dexamethasone induces endothelial caveolin-1 protein in thoracic aorta and in lung artery in healthy male rats. Thus steroids functionally attenuate endothelial responses to VEGF via caveolin-1 induction at the levels of signal transduction, migration, and tube formation, identifying a novel point of cross talk between nuclear and cell-surface receptor signaling pathways.

receptors; signal transduction; growth factors; endothelial function; angiogenesis

STEROID HORMONES THAT ACT through nuclear glucocorticoid, mineralocorticoid, and sex steroid receptors play essential roles in the maintenance of animal body homeostasis. In pathophysiological contexts, agonists for these steroid receptors are capable of exerting direct actions on cardiovascular cells, besides modulating water balance and blood pressure. For example, glucocorticoid receptor (GR) agonists downregulate endothelial nitric oxide synthase (eNOS) expression in rodent blood vessels (38) and in cultured endothelial cells (39). Clinically, hypercortisolemia in Cushing's syndrome is correlated with higher overall cardiovascular risk (26, 35) and with attenuated endothelium-dependent flow-mediated vasodilation responses in forearm arteries (1, 4). Mineralocorticoid receptor (MR) agonists also exert direct cardiovascular actions, for example, by decreasing glucose-6-phosphate dehydrogenase activity of endothelial cells (20) or by inducing eNOS "uncoupling" (28). It has clinically been known that patients suffering from primary aldosteronism exhibit a cardiovascular complication rate out of proportion to blood pressure levels seen in those suffer from essential hypertension (6). In contrast, a sex steroid 17β-estradiol increases eNOS at the levels of enzyme activity and mRNA and protein expression levels, leading to favorable outcomes on the vasculature (17). Cardiovascular actions of steroid receptor agonists may also be related to the modulation of angiogenesis, formation of new blood vessels from the preexisting ones. For example, inhaled corticosteroid effectively attenuates pathological angiogenesis in chronic airway diseases (40). Addition of corticosteroid to infantile hemangioma-derived stem cells suppresses vascular endothelial growth factor (VEGF) production, thereby leading to attenuated tumor growth in vivo (13). VEGF represents a well-characterized polypeptide growth factor acting through specific receptor tyrosine kinases expressed on the endothelial cell surface, leading to numerous responses. However, how steroids may regulate functions of vascular endothelial cells, including those modulated by VEGF, has remained incompletely understood.

In vascular endothelium, plasmalemmal caveolae, small and flask-shaped invaginations, serve as key signal transducing microdomains (30). These microdomains are enriched in various endothelial signaling proteins, including receptors such as VEGF receptor 2 (VEGFR2), protein kinases such as Akt as well as MAP kinases ERK1/2, and effector molecules such as eNOS. Caveolins are the constituent proteins of caveolae that interact with and modulate functions of caveolae-targeted proteins (30). It appeared interesting to us that some of the steroids influence the abundance of caveolin-1 isoform. For example, progesterone and testosterone increase caveolin-1 expression in breast (31) and prostate (22) cancer cells, respectively. Caveolin-1 is upregulated by the GR agonist dexamethasone in rat-derived lung epithelial cell lines (2). We therefore examined hypotheses that steroids modulate expression levels of caveolin-1 and that induction of caveolin-1 by steroids is associated with perturbed endothelial responses to VEGF.

Address for reprint requests and other correspondence: J. Igarashi, 1750-1 Ikenobe, Miki-Cho, Kita-Gun, Kagawa 761-0793, Japan (e-mail: igarashi@med.kagawa-u.ac.jp).

MATERIALS AND METHODS

Reagents. Antibodies and related compounds were commercially obtained as follows: anti-caveolin-1, anti-eNOS, and anti-ERK1/2 monoclonal antibodies were from BD Biosciences (San Jose, CA); anti-phospho VEGFR2 antibodies (Tyr1175), anti-phospho-Akt antibody (Ser473), anti-Akt polyclonal antibody, anti-phospho-eNOS antibody (Ser1179), and anti-phospho-ERK1/2 antibody (Thr202/Tyr204) were from Cell Signaling Technologies (Beverly, MA). Polyclonal antibodies directed to actin and to von Willebrand factor (vWF) were from Santa Cruz (Santa Cruz, CA). SuperBlock reagents, SuperSignal substrates for chemiluminescence detection, Restore Western Blot Stripping Buffer, and secondary antibodies conjugated with horseradish peroxidase were from Pierce (Rockford, IL). FITC-conjugated antibody to rabbit IgG, Cy3-conjugated streptavidin, and biotin-conjugated anti-mouse IgG were from DAKO (Glostrup, Denmark). TO-PRO 3 was from Invitrogen.

Bovine aortic endothelial cells (BAECs) were obtained from Cell Systems (Kirkland, WA). DMEM, LipofectAMINE 2000, and OptiMEM were from Invitrogen (Carlsbad, CA). FBS was purchased from Hyclone (Logan, CT). Human umbilical vein endothelial cells (HUVEC), HuMedia-EG2 culture medium, and tubule staining kit for CD31 were obtained from Kurabo (Osaka, Japan). Protease Inhibitor Cocktail III was from Merck (Whitehouse Station, NJ). An angiogenesis kit that contained a coculture system of HUVEC and normal human fibroblasts, supplemented with culture medium and accessory reagents, was also from Kurabo. RNeasy mini columns were from Qiagen (Valencia, CA). Taq DNA polymerase was from Promega (Madison, WI). The Rac1 activity assay kit was from Cytoskeleton (South Acoma, CO). An automated HPLC system ENO-20 was from Eicom (Kyoto, Japan). The CytoSelect 24-well cell migration assay kit (8 μm, Colorimetric Format) was from Cell Biolabs (San Diego, CA). Male Wister rats (8-wk-old) were obtained from Japan SLC (Shizuoka, Japan). A tissue-freezing medium, Tissue Tek OTC compound, was from Sakura Finetechnical (Tokyo, Japan). Protein concentration was determined by a protein assay bicinchoninate kit from Nacalai Tesque (Kyoto, Japan). All materials were from Sigma (St. Louis, MO) unless otherwise stated.

Cell culture and drug treatment. BAEC and HUVEC were maintained in culture as described previously (14, 36). HUVEC were used between passages 3 and 6. Steroids and steroid receptor antagonists were resolved into ethanol and were stored at −80°C. After reaching subconfluence, both cells were cultured in medium containing 1% of FBS for 2 days together with various drugs before being used for experiments. The final concentration of solvents did not exceed 0.1%.

RNA preparation and amplification by real-time quantitative RT-PCR. Total RNA was isolated from BAEC using the RNeasy mini column (Qiagen) (15). One microgram of total RNA was transcribed into cDNA using random hexamer and reverse transcriptase in a total volume of 20 μl. The reverse transcription was performed at 37°C for 90 min and then at 70°C for 15 min. Quantitative RT-PCR was performed by using SYBR Premix Ex Taq II system (Takara Biotechnology Shiga, Japan) and melting curve analysis using StepOne Plus Real-time PCR system (Applied Biosystems) with 18S rRNA as a reference gene. We used the Perfect real-time supporting system (Takara) to design primers specific to bovine caveolin-1 (primer set ID: BA050199) and 18S rRNA (primer set ID: BA030502). After an initial denaturation at 95°C for 30 s, amplification was performed by denaturation at 94°C for 10 s and annealing and extension at 60°C for 40 s for 50 cycles. The quantities of amplified products were monitored directly by measuring the increase of the dye intensity of the SYBR Green II (Takara) and the ROX Reference Dye (Takara). The copy number in each PCR product was defined based on a standard curve. A calibration curve was constructed by plotting the PCR threshold cycle number at which the fluorescent signal generated during the replication process passes above a threshold value against known amounts of cDNA. Caveolin-1 mRNA expression levels were normalized with 18S rRNA mRNA level.

Immunoblot analyses. Immunoblot analyses were performed as described previously (15). After being washed with ice-cold PBS, cells were harvested and lysed into cell lysis buffer containing 20 mM Tris pH 7.5, 1 mM EDTA, 1 mM EGTA, 1% Triton X-100, 150 mM NaCl, 1 mM Na_3VO_4, 2.5 mM sodium pyrophosphate, 1 mM β-glycerophosphate, and a mixture of protease inhibitors. Proteins were denatured, size-fractionated on sodium dodecyl sulfate polyacrylamide gels, and transferred to nitrocellulose membranes. The resulting membranes were blocked and incubated with various primary antibodies, followed by incubation with corresponding horseradish peroxidase-conjugated secondary antibodies, performed in TBS (pH 7.4) supplemented with 0.1% Tween-20. Immunoreactive signals were visualized using Pierce SuperSignal substrates for chemiluminescence detection with exposure to standard X-ray films (Fuji, Tokyo, Japan). In some experiments, antibodies used in the immunoblot analyses were removed from membranes using Restore Western Blot Stripping Buffer and reprobed with different antibodies.

Isolation of caveolae-enriched fractions. Caveolae-enriched fractions were separated by using ultracentrifugation with a discontinuous sucrose gradient system essentially as previously described (15, 33). Briefly, BAEC from two 100-mm dishes were scraped together into 2 ml of "carbonate buffer" containing 500 mM sodium carbonate (pH 11), 25 mM 2-(N-morpholino)ethanesulfonic acid, and 150 mM NaCl, and the cells were homogenized and sonicated. After an aliquot of whole cell lysate had been saved, the resulting cell suspension was brought to 45% sucrose (wt/vol) by addition of 2 ml of carbonate buffer containing 90% sucrose and placed at the bottom of a 12-ml ultracentrifuge tube. A discontinuous gradient was formed above the 45% sucrose bed by addition of 4 ml each of 35 and 5% sucrose solutions prepared in carbonate buffer. After centrifugation using a RPS40T rotor (Hitachi, Tokyo, Japan), 12 × 1 ml fractions were collected starting at the top of each gradient. An equal volume of each fraction was analyzed by SDS-PAGE and immunoblotting.

Transfection with small interfering RNA. BAEC were transiently transfected with 1 nM of small interfering RNA (siRNA; Ref. 15). Sequences of control and caveolin-1-specific siRNA were exactly as described previously (12, 15). Five hours after transfection, cells were recovered in a growth medium overnight. Then, they were incubated for 48 h in medium containing 1% FBS, together with either dexamethasone or vehicle.

Rac1 activity assay. Rac1 activity in BAEC was assessed as described previously (15) using a commercially available pull-down assay kit, in which GTP-bound (activated) form of Rac1 was precipitated using beads conjugated with the glutathione *S*-transferase-tagged p21-binding domain of p21 activated kinase I.

Measurement of nitrite levels in culture media. Release of nitric oxide from BAEC for 6 min after addition of VEGF was examined by measurement of nitrite accumulation in the phenol red-free culture media as described (14). The degrees of nitrite accumulation were expressed as picomoles per milligrams of protein per minute.

Cell migration assay. The migration assay used a commercially available assay kit (15). Briefly, BAEC were tripsinized and seeded onto an insert membrane in medium containing 0.4% FBS. Cells that had migrated across the membranes toward chemoattractants were stained with a blue-color dye. They were then dissolved into a lysis solution and subjected to quantification by measuring the optical density at 560 nm.

Tube formation assay. The tube formation activity of cultured endothelial cells was assessed using a commercially available coculture system of HUVEC with normal human fibroblasts as described previously (36). Ten days following incubation periods with dexamethasone (10 μM) or vehicle, endothelial cells were stained and identified with an anti-CD-31 antibody. The area of the formed tube was measured by the ImageJ program. Four pictures from each well

were provided for the estimation. Culture media and reagents were exchanged every 3 days during the assay.

Animal studies and immunofluorescence microscopy. Immunostaining was performed as described previously (41). Twelve of the 8-wk-old male Wistar rats were housed one rat per cage with temperature and light control (25°C and 12:12-h light-dark cycle). Six each of them were intraperitoneally injected with dexamethasone (0.1 mg·kg body wt^{-1}·day^{-1}) or equivalent volume of ethanol in every morning, respectively. They were killed exactly 48 h after the initial dexamethasone administration using pentobarbital (50 mg/kg body wt ip injection). All rat lung and descending aorta tissues were embedded in a tissue-freezing medium and frozen in liquid nitrogen. Cryostat sections were incubated with primary antibodies overnight at 4°C, and the immunoreactive signal was detected with FITC-conjugated antibody to rabbit IgG or a combination of Cy3-conjugated streptavidin and biotin-conjugated anti-mouse IgG. TO-PRO-3 was used for nuclear detection. Immunofluorescent images were viewed with LSM 700 confocal laser microscope (Carl Zeiss, Jena, Germany). Immunoreactive signals corresponding to endothelial caveolin-1 in a given slice derived from either thoracic aorta or from lung artery were captured using a fluorescent microscope BioRevo BZ9000 (Keyence, Tokyo, Japan) and were quantified using the Keyence software, Dynamic Cell Count. These experimental protocols conformed to the *Guide for the Care and Use of Laboratory Animals*, published by the National Institutes of Health (NIH Publication No. 85–23, revised 1996) and were approved by the Institutional Animal Care and Use Committee of Kagawa University.

Other methods. All cellular experiments were performed at least three times. Mean values for individual experiments are expressed as means ± SE. Statistical differences were analyzed by ANOVA followed by Scheffé's F test or by Student's t-test where appropriate using Statcel3 (OMS, Saitama, Japan). A P value <0.05 was considered statistically significant.

RESULTS

We started our exploration by treating BAEC, an archetypal model of endothelial cell culture, with dexamethasone, a synthetic GR agonist. Quantitative RT-PCR assays revealed that dexamethasone (for 48 h) led to dose (Fig. 1*A*)- and time (Fig. 1*B*)-dependent increases in caveolin-1 mRNA abundance. We also subjected the same cDNA templates to conventional semiquantitative RT-PCR assays and obtained similar results that caveolin-1 mRNA abundance was augmented with dexamethasone treatment (data not shown). Additionally, we noted that dexamethasone did not alter the amounts of BAEC transcripts that encode GAPDH. We next studied the effects of dexamethasone on caveolin-1 protein amounts. Dexamethasone induced a dose-dependent upregulation of caveolin-1 at a level of protein expression (Fig. 2). We tested the effects of several other steroid receptor agonists and found that aldosterone, a MR agonist, but not the sex steroids 17β-estradiol, testosterone, or progesterone, elicited induction of caveolin-1 protein albeit to a lesser extent than does dexamethasone (Fig. 2). Not only dexamethasone but also cortisol and corticosterone, which represent endogenously produced glucocorticoids in various animal species (10), similarly upregulated caveolin-1 abundance in BAEC (data not shown).

Because caveolin-1 protein undergoes a variety of posttranslational modifications including oligomerization and translocates to caveolae microstructures of peripheral plasma membrane (reviewed in Ref. 7), it was of interest to explore whether or not caveolin-1 is properly targeted to caveolae-enriched fractions even after being upregulated by dexamethasone. For this sake, we performed a well-established detergent-free subcellular fractionation protocol with a discontinuous sucrose density system (33) to analyze BAEC lysates (15) with or without dexamethasone. The results indicate that caveolin-1 signals were detected only at the interface between 5 and 35% sucrose solutions, which represent caveolae-enriched fractions

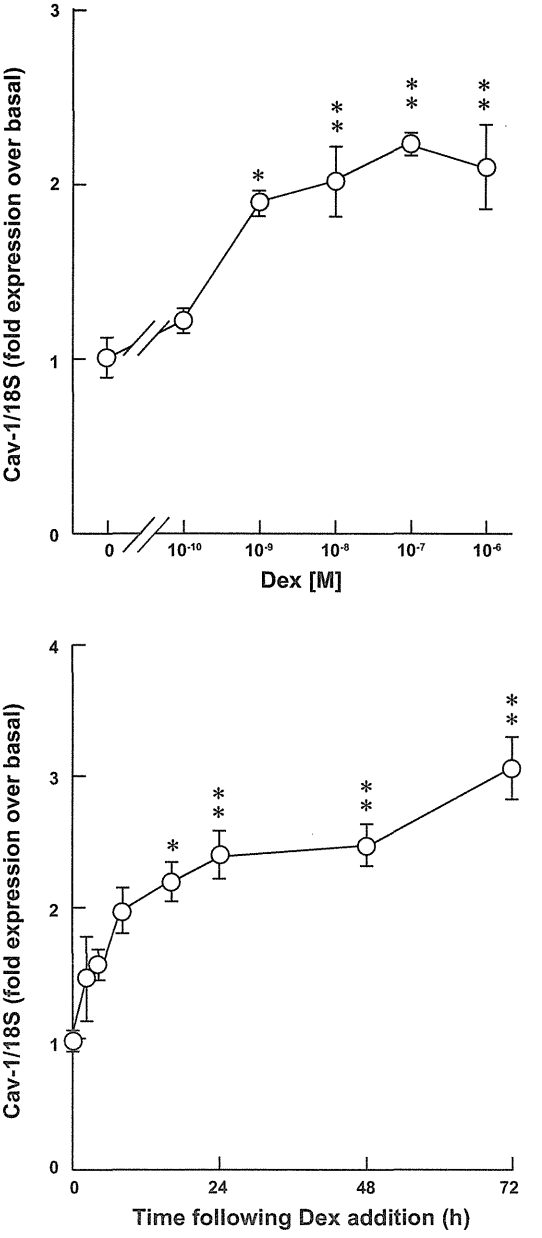

Fig. 1. Effects of dexamethasone on caveolin-1 mRNA abundance in bovine aortic endothelial cells (BAECs). Shown are the results of quantitative (q)RT-PCR assays. BAEC were treated with dexamethasone (Dex) either at the indicated concentration for 48 h (*A*) or at 1 μM for the times indicated (*B*), followed by RNA isolation. Reverse-transcribed template cDNA samples were subjected to qRT-PCR using the primers specific to bovine caveolin-1 (Cav-1) as well as 18S. Each data point represents the fold increase in transcript expression levels of Cav-1 relative to those of 18S, normalized to the values obtained from the cells before stimulation with Dex. $*P < 0.05$ and $**P < 0.01$ vs. cells treated with vehicle alone; $n = 4$ and 6 in *A* and *B*, respectively.

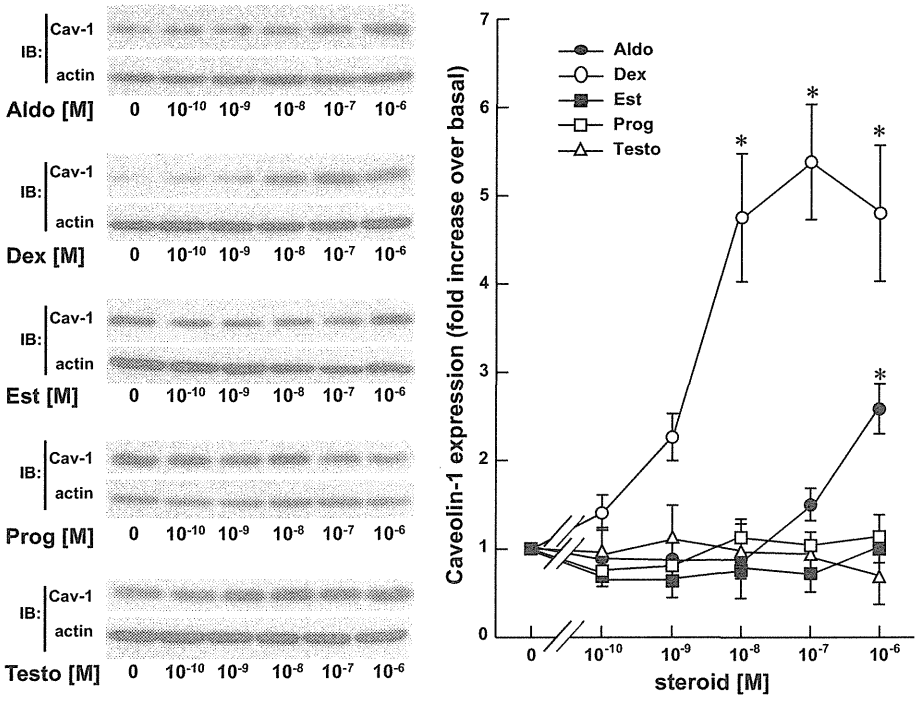

Fig. 2. Effects of various steroids on caveolin-1 protein abundance in BAEC. Shown are the results of immunoblot assays using lysates derived from BAEC treated with various steroid hormones (Aldo, aldosterone; Dex, dexamethasone; Est, 17β-estradiol; Prog, progesterone; Testo, testosterone; at the indicated concentrations for 48 h, respectively; IB, immunoblot). Cellular proteins were probed with antibodies directed to Cav-1 and actin. *Left*: data are representative of 4 independent experiments that yielded equivalent results. *Right*: results of densitometric analyses from pooled data, plotting the fold increase of the degree of expression levels of caveolin-1 at the indicated time point, relative to the signals obtained in the absence of steroids. $*P < 0.05$ vs. cells treated with vehicle alone.

(Fig. 3*A*). Thus caveolin-1 seems to be targeted to caveolae-like fractions even in the presence of dexamethasone after undergoing similar post-transcriptional modifications with vehicle-treated cells. We then performed a time-course assay in which BAEC were treated with 1 μM of dexamethasone for various time points, followed by immunoblot analyses. Results indicate that dexamethasone led to time-dependent increases in caveolin-1 protein abundance (Fig. 3*B*). Expression levels of several other endothelial proteins, including actin, VEGFR2, eNOS, protein kinases ERK1/2 as well as Akt, a small G-protein Rac1, did not change over these dexamethasone treatment protocols (see Figs. 3*B*, 4, and 5). We tested whether or not RU-486, a GR antagonist, and spironolactone, a MR inhibitor, counteracts steroids-induced upregulation of caveolin-1 protein in BAEC. Dexamethasone and aldosterone at 1 μM increased the abundance of caveolin-1 to the similar degrees as we observed in Fig. 2; however, promotion of caveolin-1 expression was not seen in the presence of RU-486 and spironolactone, respectively (Fig. 4, *A* and *B*). Collectively, these results serve to demonstrate that agonists for GR and MR, but not those for sex steroid receptors, are capable of upregulating the expression of caveolin-1 at the levels of protein and mRNA in BAEC.

Caveolin-1 is a key scaffolding protein of caveolae microdomains that modulates amplitudes of endothelial cell responses to various extracellular stimuli, including polypeptide growth factors such as VEGF (19). We therefore explored functional consequences of steroid induction of caveolin-1. We examined various responses of BAEC to VEGF that had been treated with or without dexamethasone for 48 h. We first examined the protein phosphorylation responses. As shown in Fig. 5*A*, the degrees of VEGF-promoted protein phosphorylation in VEGFR2 (Tyr1175), kinases Akt (Ser473), ERK1/2 (Thr202/Tyr204), and eNOS (Ser1179) were markedly attenuated in cells pretreated with dexamethasone that expressed higher amounts of caveolin-1 protein. When dexamethasone-elicited induction of caveolin-1 protein had been pharmacologically counteracted by RU-486, attenuation of these phosphorylation responses to VEGF was reversed (Fig. 5*B*). We also took genetic knockdown approach using previously established siRNA specific to bovine caveolin-1 (12) in combination with dexamethasone. When upregulation of caveolin-1 protein by dexamethasone was abrogated by siRNA transfection, attenuation of phosphorylation responses in VEGFR2, Akt ERK1/2, and eNOS proteins were completely recovered (Fig. 5*C*), although neither treatment with dexamethasone nor transfection with caveolin-1 siRNA affected abundance of total VEGFR2, Akt ERK1/2, or eNOS. Thus ability of dexamethasone to attenuate VEGF-elicited protein phosphorylation responses derives from upregulation of caveolin-1. Rac1 is a small G-protein that plays a pivotal role in mediating VEGF signaling pathways (11). Figure 6*A* indicates that Rac1 activation by VEGF was reduced in dexamethasone-pretreated cells compared with vehicle. eNOS is a downstream effector that is activated by VEGF under the control of upstream protein kinases and small G proteins (21). Figure 6*B* shows that stimulation with VEGF led to higher levels of nitric oxide production and that pretreatment with dexamethasone markedly abrogated it. When induction of caveolin-1 by dexamethasone was inhibited by siRNA transfection, attenuation of VEGF-elicited nitric oxide production was markedly counteracted (Fig. 6*C*). These data indicate that dexamethasone, which elevates caveolin-1 abundance, attenuates VEGF-activated signal transduction pathways at multiple levels including protein phosphorylation, Rac1 activation, as well as eNOS activation.

Migration and tube formation of endothelial cells in response to VEGF represent important physiological steps

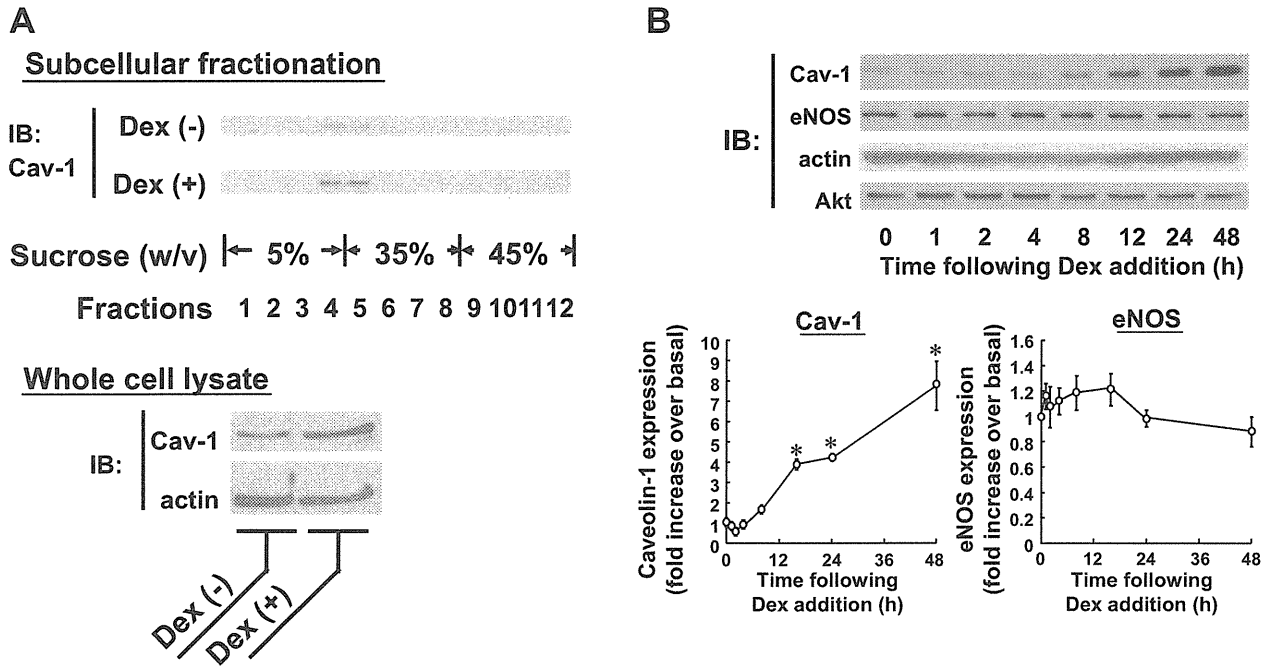

Fig. 3. Characterization of dexamethasone-induced upregulation of caveolin-1 protein abundance in BAEC. *A*: results of subcellular fractionation assay of BAEC treated with or without Dex (at 1 μM for 48 h). Sonicated cell lysates from BAEC were separated using a discontinuous sucrose gradient system as described in MATERIALS AND METHODS. An equal volume from each fraction was separated by SDS-PAGE, followed by immunoblot analysis using an antibody directed against caveolin, as indicated at *top*. An aliquot of whole cell lysate had been withdrawn before subcellular fractionation and was separately subjected to immunoblots as shown at *bottom*. Shown are representative of 3 independent experiments that yielded equivalent data. Note that Cav-1 protein in both vehicle- and Dex-treated BAEC was specifically recovered at the interface between the 5% and 35% sucrose gradient, representing the caveolae-enriched fractions. *B*: results of time course assay in which BAEC were treated with 1 μM of Dex for the indicated durations. Cellular proteins were probed with antibodies directed to Cav-1, endothelial nitric oxide synthase (eNOS), actin, and Akt. *Top*: data are representative of 4 independent experiments that yielded equivalent results. *Bottom*: results of densitometric analyses from pooled data, plotting the fold increase of the degree of expression levels of Cav-1 and eNOS at the indicated time point, relative to the signals obtained in the absence of dexamethasone. $^*P < 0.05$ vs. cells treated with vehicle alone.

during angiogenic processes evoked by the growth factor (29). Using a modified Boyden chamber assay, we found that BAEC preexposed to dexamethasone exhibited lower magnitudes of migration both toward VEGF and toward serum (Fig. 7, *A* and *B*). We sought to explore the effects of dexamethasone in a human-derived endothelial cell culture model, HUVEC. Dexamethasone led to time-dependent augmentation of caveolin-1 protein abundance in HUVEC monoculture (Fig. 7*C*). Unlike in BAEC, dexamethasone attenuated eNOS protein expression. After confirming that dexamethasone induces caveolin-1 in HUVEC, we explored the effects of dexamethasone in tube forming activity using a commercially available and previously established coculture system of HUVEC with normal human fibroblasts (36). In this system, cells were incubated for 10 days in the presence and absence of dexamethasone. The degrees of endothelial tube formation were determined by means of immunostaining using an anti-CD31 antibody. Figure 7*D* indicates that the magnitude of tube formation by HUVEC in the presence of dexamethasone markedly decreased to approximately half of that seen with the vehicle. Together, these results demonstrate that endothelial cells pretreated with dexamethasone that express higher amounts of caveolin-1 exhibit attenuated responses to VEGF not only at the level of signal transduction but also at more distal levels of motility, i.e., migration and tube formation.

To explore whether or not steroids are able to upregulate caveolin-1 protein expression in vascular endothelium of living animals, we isolated thoracic aorta and lung tissues from normal male rats treated with or without dexamethasone and double-stained them with anti-caveolin-1 and anti-vWF antibodies. Caveolin-1 distributed in aorta and lung arterial cells (Fig. 8). When dexamethasone was applied for 2 days, enhanced expression of caveolin-1 was observed. Quantitative microscopic analyses revealed that endothelial caveolin-1 immunoreactive signals significantly increased by 63 ± 29% in thoracic aorta ($P < 0.05$ vs. vehicle) and tended to increase by 62 ± 13% in lung artery ($P < 0.1$). In contrast, expression of vWF of endothelial cells did not change at before and after dexamethasone treatment. These data indicate that the expression of caveolin-1 is upregulated at both aorta and lung arterial endothelial cells after dexamethasone treatment in living animals as well as in cultured endothelial cells. When whole tissue extracts were analyzed for caveolin-1 mRNA (lung and aorta, conventional RT-PCR) and protein (lung, immunoblot), we did not observe differences between dexamethasone- vs. vehicle-treated animals (data no shown). These results suggest that caveolin-1 induction by dexamethasone under these stimulation protocols occurred specifically in vascular endothelium, rather than taking place in the bulk of cell types.

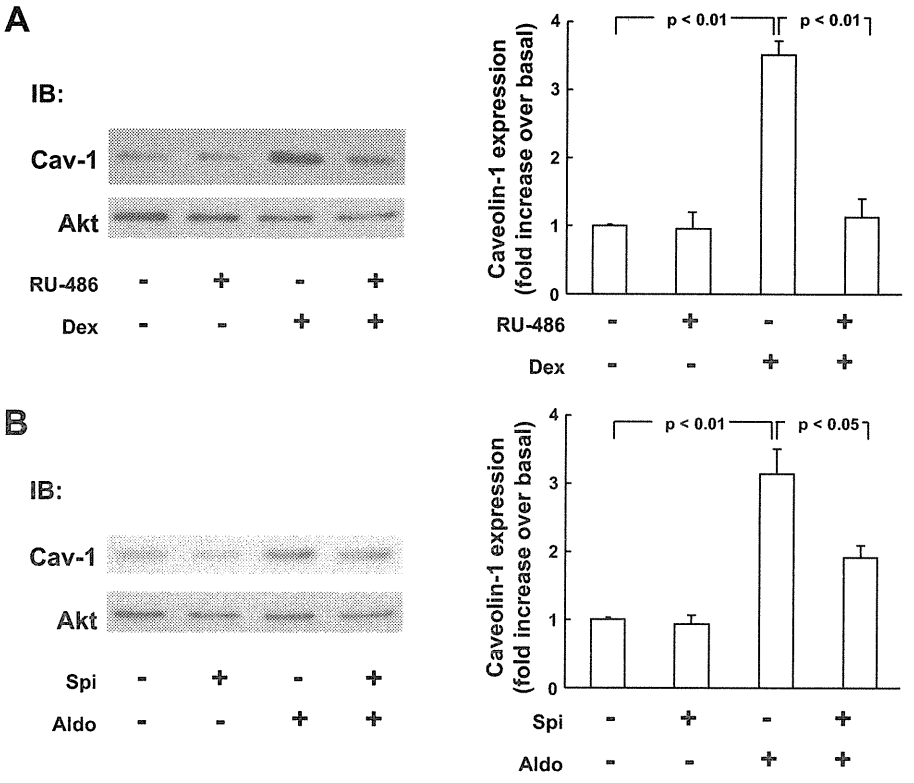

Fig. 4. Effects of steroid receptor antagonists on caveolin-1 upregulation induced by dexamethasone and aldosterone. *A*: results of protein immunoblot analyses in which effects of RU-486, a glucocorticoid receptor (GR) inhibitor, on Dex-mediated upregulation of endothelial Cav-1 protein abundance were examined. BAEC had been treated with RU-486 (1 μM for 30 min) or vehicle; an aliquot of Dex stock solution (or vehicle) was then added to the cultures to achieve a final concentration of 1 μM, as indicated. Incubation proceeded further for 48 h and protein samples were harvested and subjected to immunoblot analyses as above. *Left*: representative images. *Right*: results of densitometric analyses from pooled data, plotting the fold increase of the degree of expression levels of Cav-1, relative to the signals obtained in the absence of Dex and RU-486. *B*: spironolactone (Spi), a mineralocorticoid receptor inhibitor, and Aldo (both at 1 μM) were employed instead of RU-486 and Dex; $n = 4$ in *A* and *B*.

DISCUSSION

These results have demonstrated, for the first time to our knowledge, that the expression levels of caveolin-1 mRNA and protein in vascular endothelial cells are subjected to dynamic regulation by treatment with steroid agonists for GR and MR, associated with attenuated responses to VEGF. Induction of caveolin-1 by dexamethasone was observed in the endothelial cells derived from three independent experimental models, BAEC, HUVEC, as well as blood vessel preparations isolated from normal male rats. Furthermore, these responses took place within pharmacologically relevant drug concentrations, suggesting that caveolin-1 can be induced by steroids in multiple types of vascular endothelial cells in various experimental settings. RU-486 and spironolactone are capable of counteracting caveolin-1 induction by dexamethasone and by aldosterone, while three other sex steroids tested are without effect. Thus the abilities of steroids to augment caveolin-1 expression seem to be limited to GR and MR, but not sex steroid receptor, agonists. Caveolin-1 is known to be rather down-regulated in vascular endothelial cells by several other extracellular stimuli including cytokines and pharmacological agents (8, 15, 23). Although a glucocorticoid receptor element-like sequence has been identified at ~1,526-bp upstream of mouse caveolin-1 gene (37), the functions of these genomic elements are not currently known in endothelial cells. There remains the possibility that steroids modulate caveolin-1 expression at the levels other than transcription for example by translation, posttranscription, or degradation pathways (reviewed in Ref. 7). Some sex steroids are capable of modulating caveolin-1 expression in several nonendothelial cell types, for example, in breast (31) as well as in prostate (22) cancer cells. Thus precise molecular mechanisms whereby steroids regulate caveolin-1 expression, which are beyond the scope of current studies, remain to be elucidated both in endothelial- and nonendothelial cells.

Dexamethasone upregulates caveolin-1 in rat-derived lung epithelial cell lines (2) and in pancreatic acinar cells (24). Adipocytes express dramatically higher levels of caveolin-1 when differentiated by a hormonal mixture including dexamethasone (32). Thus these earlier observations indicate that glucocorticoid-induction of caveolin-1 is not limited to vascular endothelial cells. However, our data indicate that in whole rat organ homogenates expression levels of caveolin-1 mRNA (lung and aorta) and protein (lung) do not change 48 h after dexamethasone (data not shown), suggesting that dexamethasone does not largely affect caveolin-1 abundance in nonendothelial cell types under current protocols. Notably, functional consequences of caveolin-1 upregulation by steroids have remained completely unexplored in any cell types. We therefore sought to determine if dexamethasone leads to perturbed responses of vascular endothelial cells to extracellular stimuli. We focused on VEGF because this angiogenic growth factor represents a pivotal regulator of endothelial functions (29) and because VEGF receptor signaling is modulated by caveolae microdomains and caveolins (19, 23). VEGF activates a wide array of endothelial signal transduction pathways, starting from activation/phosphorylation of cognate receptor tyrosine kinases (VEGFR2), activation/phosphorylation of downstream protein kinases including Akt and ERK1/2, activation of a key small G-protein Rac-1, as well as eNOS-dependent nitric oxide production associated with Akt-mediated phosphorylation of

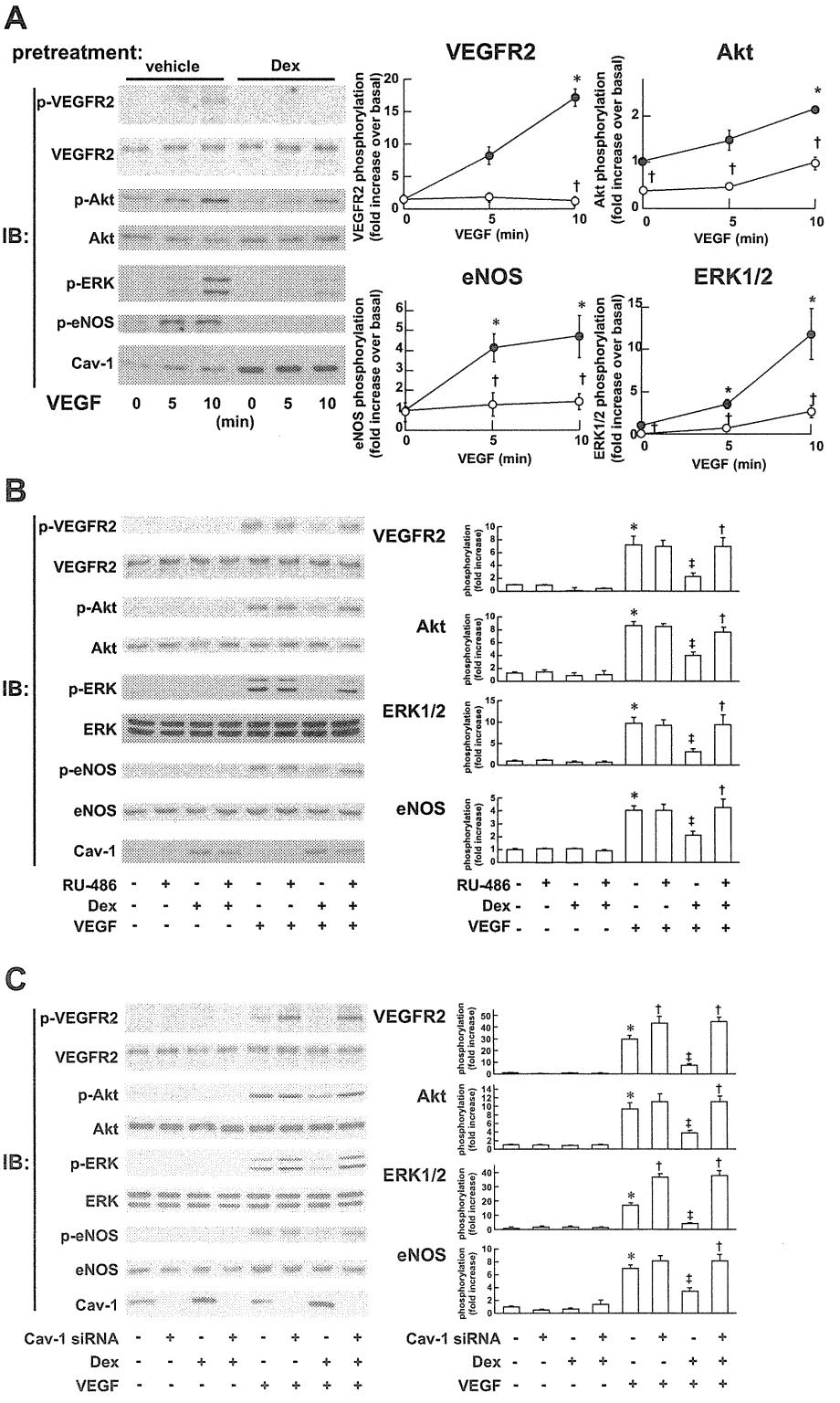

Fig. 5. Effects of dexamethasone, RU-486 and caveolin-1 specific small interfering (si)RNA on VEGF-elicited phosphorylation responses in BAEC. *A*: results of a protein immunoblot assay analyzed in cell lysates derived from BAEC treated with Dex followed by VEGF. BAEC had been incubated with Dex (1 μM for 48 h) or vehicle and then they were treated with VEGF (5 ng/ml). Following treatment with VEGF for the times indicated, cellular proteins were subjected to immunoblot assays, probed with antibodies directed to phospho-VEGFR2 (Tyr 1175), phospho-Akt (Ser473), phospho-eNOS (Ser1179), phospho-ERK1/2 (Tyr202/Thr204), and Cav-1. Equal loading of samples was confirmed by reprobing the immunoblots with antibodies against (total) VEGFR2 and Akt. *Left*: representative images. *Right:* results of densitometric analyses from pooled data, plotting the fold increase of the degree of phospho-proteins normalized to the values obtained in the absence of VEGF and Dex. Open and closed circles represent values obtained with and without pretreatment with Dex, respectively. $*P < 0.05$ vs. VEGF (−). †$P < 0.05$ vs. Dex (−); $n = 4$. *B*: cells had been pretreated with RU-486 and/or Dex (as in Fig 4*A*), followed by VEGF (5 ng/ml for 10 min). After the addition of VEGF, cells were harvested and subjected to immunoblot assays, using antibodies directed to phospho (or total)-VEGFR2, phospho (or total)-Akt, phospho (or total)-eNOS, phospho (or total)-ERK1/2, and (total) Cav-1. Pooled data of densitometry are presented in the right half, normalizing the values to those obtained in the absence of RU486, Dex and VEGF. $*P < 0.05$ vs. VEGF (−). †$P < 0.05$ vs. RU486 (−). ‡$P < 0.05$ vs. Dex (−); $n = 4$. *C*: BAEC were transfected with either control siRNA [indicated as Cav-1 siRNA (−)] or that directed to caveolin-1 [Cav-1 siRNA (+)] before dexamethasone (1 μM for 48 h) followed by VEGF (5 ng/ml for 5 min). Cells were then subjected to immunoblot analyses and densitometry as above, normalizing the values to those obtained in the absence of Dex and VEGF in control siRNA-treated cells. $*P < 0.05$ vs. VEGF (−). †$P < 0.05$ vs. control siRNA. ‡$P < 0.05$ vs. Dex (−).

eNOS protein. Our results show that when endothelial cells express higher amounts of caveolin-1 protein due to dexamethasone, these signaling events are alike attenuated. In these experiments we focused on one micromolar of dexamethasone, which has been frequently used in various cells cultures (5, 39), so as to ensure maximum caveolin-1 induction and inhibition on VEGF responses. Conversely, RU-486, a pharmacological GR antagonist, as well as transient transfection with caveolin-

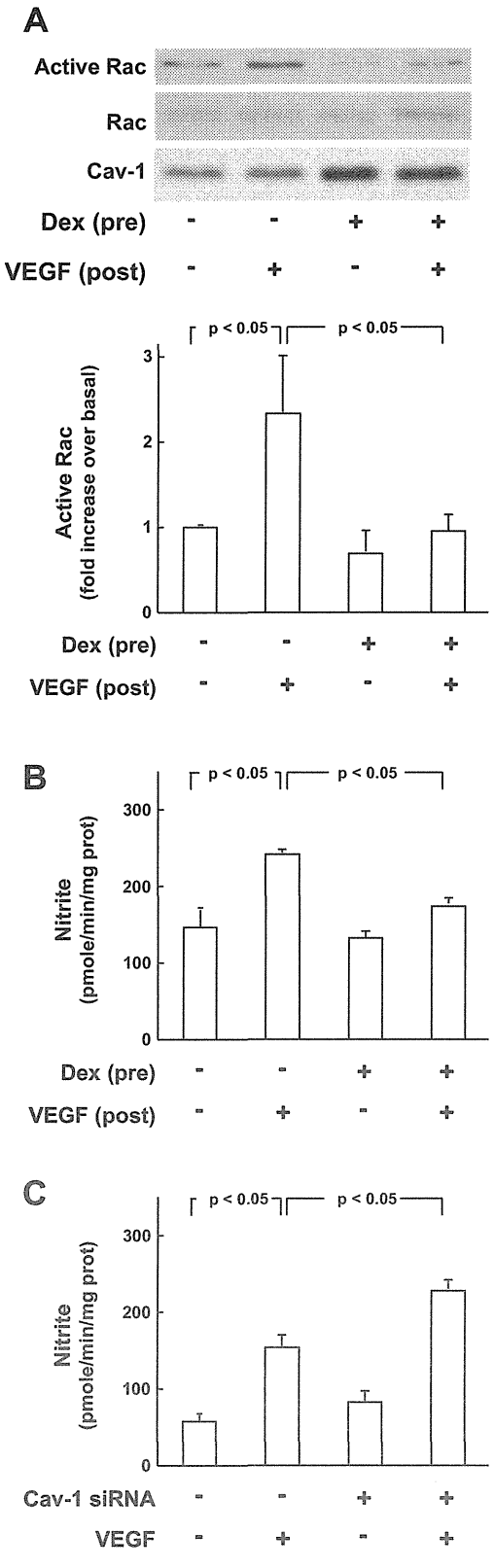

1-specific siRNA, counteracts attenuation of protein phosphorylation responses to VEGF induced by dexamethasone, concomitantly with decreases in caveolin-1. Caveolin-1 protein is supposed to be specifically targeted to plasmalemmal caveolae after completing its oligomerization processes (7). Our subcellular fractionation assays revealed that the caveolin-1 protein in BAEC is specifically targeted to caveolae-enriched fractions regardless of dexamethasone treatment. Thus the steroid agent appears to alter VEGF responses primarily by augmenting the abundance of caveolin-1 protein rather than by influencing its subcellular location and/or oligomerization status. An earlier report shows that in heterologous expression systems of 293T human fibroblast cell line, caveolin-1 acts as a direct negative regulator of VEGFR2 tyrosine kinase (19). Caveolin-1 also plays inhibitory roles in VEGF signal transduction pathways at the level of eNOS enzyme (27) and at that of upstream Rac1-Akt signaling axis (11, 12, 21). Endothelial-specific overexpression of caveolin-1 leads to impaired vascular permeability and angiogenic responses to VEGF in mice (3). When taken together with these earlier observations, the present results are consistent with a hypothesis that it is the abundance of caveolin-1 protein that plays a major role to determine the amplitudes of endothelial signaling responses to VEGF, under the control of nuclear steroid receptors. In a broader perspective, however, the roles of caveolin-1 in modulating the cellular signal transduction pathways appear to be highly complex and context dependent. For example, a stable knockdown of caveolin-1 in NIH-3T3 cells leads to augmented ERK1/2 activation (9). In contrast, in cultured endothelial cells derived from caveolin-1 null mice, VEGF-induced ERK1/2 phosphorylation responses are abrogated, rather than hyperactivated (34). Although our results are in line with the former example, these earlier studies suggest that one needs a caution in extrapolating the findings obtained in a given cellular system to the other in terms of caveolin-1 actions on receptor signal transduction pathways.

We have tested the effects of dexamethasone on migration as well as tube formation, both representing key angiogenic processes of vascular endothelial cells. Modified Boyden chamber assay revealed that cells pretreated with dexamethasone that express more abundant caveolin-1 protein display significantly lower degrees of migratory responses evoked both by VEGF and by 10% FBS in BAEC, suggesting that upregulation of caveolin-1 by dexamethasone is associated with perturbed migration toward VEGF and also likely toward some other migratory response-related bioactive substances included in the FBS. By using a previously

Fig. 6. Effects of dexamethasone on VEGF-elicited Rac1 activation and nitric oxide production in BAEC. *A*: results of Rac1 activity assay. BAEC had been incubated with Dex (1 μM for 48 h) or vehicle, then they were treated with VEGF (10 ng/ml for 1 min). Rac activity in the cell lysate was measured by means of pull-down of GTP-bound Rac1. Precipitated Rac1 was quantified in immunoblots probed with a specific monoclonal antibody. Aliquots of total cell lysates were subjected to immunoblots in separate gels using antibodies specific to Rac1 and Cav-1, as indicated; $n = 3$. *B* and *C*: results of nitrite measurement. *B*: BAEC were treated with VEGF (10 ng/ml for 6 min); some cells had been pretreated with Dex (1 μM for 48 h). Culture media were then collected and subjected to nitrite measurement as described in the text; $n = 4$. *C*: BAEC had been transfected with either control or Cav-1 specific siRNA, indicated as Cav-1 siRNA (−) or (+), respectively, before being treated with VEGF. $n = 5$.

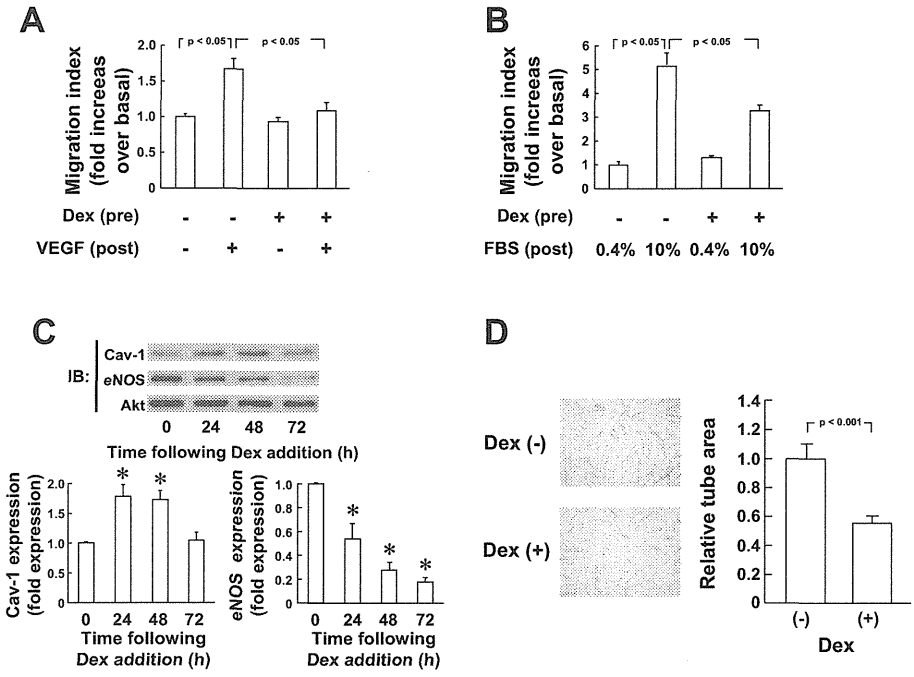

Fig. 7. Effects of dexamethasone on migratory responses in BAEC and caveolin-1 expression and tube formation activity in human umbilical vein endothelial cells (HUVEC). *A* and *B*: results of cell migration assay. BAEC had been pretreated with Dex (1 μM) or vehicle for 48 h. Then, they were trypsinized and applied for cell migration assay as described in the text. Cells were stimulated with 10 ng/ml of VEGF for 6 h (*A*) or different concentrations of FBS for 4 h (*B*) in the outer chamber during migration assay. The degrees of cell migration across the filter membranes were assessed as optical density at 560 nm, normalized to the values obtained in the absence of Dex and VEGF (*A*) or in the presence of 0.4% FBS alone (*B*), and expressed as fold increase over basal (migration index); $n = 3$, respectively. *C*: immunoblot analyses were performed in HUVEC monoculture that had been treated with Dex. Cells were treated with Dex (1 μM) for the times indicated. *Top*: representative immunoblots probed using antibodies as illustrated. *Bottom*: graphs show the results of densitometric analyses from pooled data, plotting the fold increases in expression levels of caveolin-1 and eNOS at the indicated Dex treatment duration, relative to the signals obtained in the absence of Dex; $n = 6$. $^*P < 0.05$ vs. cells not treated with dexamethasone. *D*: tube formation assay was performed using a coculture system of HUVEC and normal human fibroblasts. Endothelial cells were identified using an CD-31 antibody 10 days after the incubation with Dex (10 μM) or vehicle. *Left*: typical microphotogram depicting attenuated tube formation in the presence of dexamethasone (*bottom*) compared with vehicle (*top*). Tube area was estimated from 4 pictures from each well and the area of the formed tube was represented as a relative value to that formed in the wells with vehicle control. Pooled results obtained from 6 independent experiments are summarized at *right*.

established coculture model of HUVEC with normal human fibroblasts, we showed that incubation of these cells with dexamethasone for 10 days leads to attenuated endothelial tube formation activity, identified with an anti-CD31 antibody. Our earlier experiments suggested that VEGF receptor ligands endogenously secreted by adjacent fibroblasts in coculture play a significant role to promote tube formation of HUVEC in this system (36). When taken together with the fact that dexamethasone is capable of increasing caveolin-1 abundance in HUVEC monoculture, reaching to the maximum level 2 days after drug addition, our data support a hypothesis that attenuation of tube formation in HUVEC by dexamethasone occurs due to increases in caveolin-1 abundance that affects VEGF pathways. We cannot rule out the possibility that the regulatory pattern of caveolin-1 abundance in dexamethasone-treated HUVEC in coculture exhibits somewhat different kinetics compared with those actually examined in monoculture in this study, although we added fresh dexamethasone every 3 days during the tube formation assay. Plausibly, steroids, especially corticosteroids, are associated with attenuated degrees of VEGF-induced angiogenic responses in humans (13) and in experimental animal models (16, 25). Serum VEGF levels are elevated in patients with Cushing's syndrome when compared with those suffer from essential hypertension (18), suggesting some functional linkages of VEGF and steroid pathways in humans. We propose that regulation of caveolin-1 abundance by nuclear steroid receptor pathways may uncover a novel mechanism at which exposure to excess steroids, including agonists for GR and MR, leads to perturbed sensitivities of vascular endothelium to angiogenic growth factors such as VEGF. Although our experiments using normal male rats demonstrate that administration with a GR agonist can upregulate caveolin-1 in living animals, it remains to be seen if this were the case with human subjects.

In these experimental settings, expression levels of several other proteins including actin, VEGFR2, Akt, ERK1/2, and Rac1 did not change over various stimulation protocols with steroid receptor agonists, suggesting that steroid induction of endothelial caveolae-related proteins is relatively specific to caveolin-1. In some immunoblot assays we exploited Akt as a loading control because in these panels we performed phospho-Western analyses of this protein, because steroids did not alter its expression, and because the anti-Akt antibody used in this study yielded relatively strong and specific immunoreactive signals in our system. As to eNOS, dexamethasone leads to significant down-regulation of its protein expression level in HUVEC, although it does not do so in BAEC. This implies that

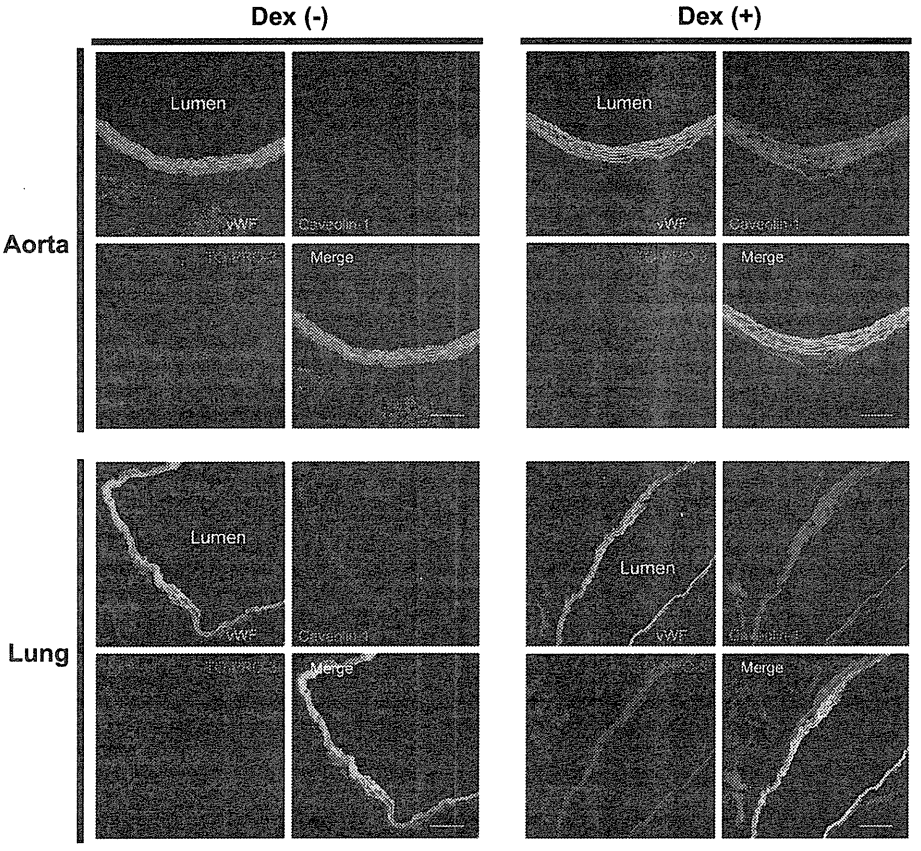

Fig. 8. Effects of dexamethasone on caveolin-1 expression in rat aortic endothelium. Shown are the representative double staining experiments with anti-von Willebrand factor (vWF) antibody (green fluorescence) and anti-caveolin-1 antibody (red fluorescence) of thoracic aorta and lung arterial cells. TO-PRO-3 was used for nuclear detection (blue fluorescence). Forty-eight hours after intraperitoneal injection of dexamethasone (0.1 mg kg/body wt), upregulation of caveolin-1 expression was observed in aorta and lung arterial cells. Scale bars = 100 μm; n = 6.

regulation of eNOS expression levels by steroids takes place on an endothelial cell subtype-specific fashion. Nonetheless, BAEC preexposed to dexamethasone exert attenuated levels of VEGF-stimulated nitric oxide production compared with vehicle control cells, despite total eNOS protein expression levels being constant. Earlier studies provided several other mechanisms whereby steroids may lead to dysfunction of eNOS system. These include down-regulation of eNOS mRNA/protein (38, 39), tetrahydrobiopterin insufficiency leading to eNOS "uncoupling" (28), or down-regulation of glucose-6-phosphate dehydrogenase activity (20). Thus our results may now identify an additional point of regulation at which these steroid receptor agonists decrease nitric oxide production even at the situation where they do not alter total eNOS abundance, provided that caveolin-1 has been established as a key inhibitory binding partner of eNOS protein (27). In our system, simple transfection with caveolin-1 specific siRNA did not increase basal NO production with a statistical significance. This may be due to the degrees of caveolin-1 protein knockdown, the sensitivity of our detection method, or some other experimental conditions.

In summary, we have demonstrated that pharmacologically relevant doses of GR and MR agonists induce caveolin-1, a major regulatory protein of plasmalemmal caveolae, in cultured vascular endothelial cells. Cells pretreated with dexamethasone that express higher levels of caveolin-1 exhibit attenuated responses to a polypeptide growth factor VEGF at the levels of signal transduction, cell migration, and tube formation. We propose that steroid-induced upregulation of caveolin-1 identifies a novel point of control at which ligands for nuclear receptors modulate signal transduction pathways activated by cell surface receptors in vascular endothelium. Because treatment with dexamethasone appears to augment caveolin-1 expression in vascular endothelium in living animals as well, our study may also provide another mechanism underlying cardiovascular disorders associated with perturbation of steroid hormone systems.

ACKNOWLEDGMENTS

We thank Toshitaka Nakagawa and Miyako Daike (Kagawa University) for superlative technical assistance.

GRANTS

This study was supported in part by a Grant-in-Aid for Scientific Research (C) to J. Igarashi (21590933) and to Y. Kubota (24591654) from the Ministry of Education, Culture, Sports, Science and Technology of Japan.

DISCLOSURES

No conflicts of interest, financial or otherwise, are declared by the author(s).

AUTHOR CONTRIBUTIONS

Author contributions: J.I. conception and design of research; J.I., T.H., K.S., K.Y., I.T., T.M., and H.K. performed experiments; J.I. and T.H. analyzed data; J.I., Y.K., and H.K. interpreted results of experiments; J.I., K.Y., and I.T. prepared figures; J.I. and K.Y. drafted manuscript; J.I. and T.H. edited and revised manuscript; J.I., T.H., K.S., K.Y., I.T., Y.K., and H.K. approved final version of manuscript.